Magnetic Sources in the Earth's Mantle

Eric C. Ferré[1], Ilya Kupenko[2], Fátima Martín-Hernández[3], Dhananjay Ravat[4], and Carmen Sanchez-Valle[2]

[1] School of Geosciences, University of Louisiana at Lafayette, Lafayette, Louisiana, U.S.A.

[2] Institut für Mineralogie, University of Münster, Münster, Germany

[3] Departamento de Física de la Tierra y Astrofísica, Universidad Complutense de Madrid, Madrid, Spain

[4] Department of Earth and Environmental Sciences, University of Kentucky, Lexington, Kentucky, U.S.A.

Abstract - When the Magsat satellite was launched back in 1979, the mantle was considered free of ferromagnetic minerals and too hot for such phases to carry any magnetic remanence. This non-magnetic mantle model influenced our interpretation of aeromagnetic and satellite data for decades. Forty years later, new experimental data, measurements on mantle xenoliths, and improved estimates for the base of the magnetized layer show the urgency to revisit this issue. Experiments on hematite and its polymorphs suggest that they could carry a magnetic remanence down to ~600 km depth, for example in cold subducted slabs. New magnetic data on a large worldwide collection of mantle xenoliths show that pure magnetite is common in the uppermost mantle (< 150 km), particularly in subduction zones and cratons. Finally, modern spectral analysis of aeromagnetic data establishes that a magnetized layer exists below the crust-mantle boundary in multiple tectonic settings. In this review, we examine the xenolith record, evaluate the latest experimental advances, assess detection methods of deep-seated mantle sources, and identify salient unsolved questions about magnetic sources in the mantle.

1. Introduction

Geophysicists use a whole array of geophysical methods rooted on seismic waves, heat flow, gravity magnetic and electromagnetic fields[1-3] to answer fundamental questions on the nature and evolution of the interior of the Earth. The general approach, referred to as the inverse problem, aims to reconstruct the internal composition, structure, and dynamics of our planet from extensive sets of geophysical data. These

methods led to key discoveries, such as documenting subducted slabs down to depths greater than 600 km[4] or that the mantle very slowly churns, driven by large convection cells[5]. Investigations of the Earth's magnetic field also led to major breakthrough in our understanding of the planet's dynamics, for example with the discovery of seafloor stripes[6]. Yet, the potential of magnetic methods to probe the interior of the Earth, its temperature and structure remains somewhat underappreciated. The launch of the Swarm magnetic satellite mission by the European Space Agency in 2013 marks a significant advance in this situation because the mission includes two satellites flying side-by-side and a third at a different elevation. This novel configuration provides high-precision and high-resolution data on the strength, direction and variations of the Earth's magnetic field. This mission, along with recent and critical advances in our understanding of deep-seated magnetic sources, calls for a review of what is magnetic in the mantle.

The currents of the partially-molten iron-nickel alloy in the outer core generate a non-steady electric field[7-8]. According to Maxwell's equations, the non-steady currents also produce a time-varying magnetic field. These fields substantially contribute to the Earth's electromagnetic environment. As the geodynamo process produces a substantial magnetic field, of about 25 to 65 μT at the surface[9], ferromagnetic rocks and materials acquire a magnetization in the geomagnetic field, some of which can be retained as remanent magnetization[10-11].

Remanent magnetism generally occurs due to the presence of Fe-oxide phases such as magnetite, titanomagnetite, and hematite or iron sulfides such as pyrrhotite and greigite. These minerals record a signature of the magnetic field during their formation. If temperatures remain below the magnetic transition temperature, named Curie/Néel temperature, this signature can be preserved for billions of years. When the temperature rises and approaches the transition temperature, thermal energy breaks magnetic ordering and, consequently, minerals lose their magnetization. For this reason, it has been assumed for many years that down deep in the Earth, at mantle depths, materials even if they contained magnetite cannot retain magnetization. The upper mantle lies from the bottom of the crust, at temperatures as low as 200ºC, to the top of the lower mantle (≈670 km) at ≈1,500ºC[12]. In most of this

temperature interval, remanent magnetization was previously considered null due to the low Curie/Néel and blocking temperatures of titanomagnetite and magnetite[10, 13-15].

However, new data from laboratory experiments, and mantle xenoliths, reveal that the assumption of non-magnetic mantle may not be valid. Mantle xenoliths and xenocrysts, because they are rapidly brought up to the surface of the Earth, provide constraints on the nature, abundance and properties of mineral phases present down to depths of 670 km[16-20]. In addition, laboratory experiments, conducted in high-pressure and high-temperature vessels, provide a wealth of information on the magnetic properties of minerals in the upper mantle, and reveal that magnetism may be preserved at deeper depths than previously thought[21-23].

New insights from xenoliths and laboratory experiments are critical as they provide constraints on the maximum temperature and, therefore, maximum depth of mantle magnetism, which has fundamental implications for the interpretation of satellite, airborne magnetic and deep-tow magnetic surveys (Figure 1) and could be a strategic resource for understanding the upper mantle structure in multiple geodynamic settings[24]. The magnetic anomalies from rocks arise from a very small fraction of magnetic minerals typically hundreds of ppm) and not the bulk properties of rocks (*e.g.*, density). Also, the ability of rocks to preserve the record of the geomagnetic field led to the detection of marine magnetic stripes and seafloor spreading[6], a mechanism that reverses with time unlike gravity and seismic waves. The acute dependency of magnetism on temperature, with a sharp drop of magnetization at the Curie temperature, makes it an important tool to understand temperature-dependent processes. Thus, magnetism informs on the geometry of isotherms and correlated plate tectonic processes. The determination of the Curie depth has also been used to assess heat flow in regions where experimental data is not available[25]. Finally, investigations also contribute to a better understanding of intriguingly large magnetic anomalies on Mars and their significance.

In this review we consider the presence and origin of potentially magnetic minerals both in the oceanic and continental lithospheric mantle, we discuss cutting-edge experiments on magnetic phases likely to be present at great depth in the mantle and show the power of modern spectral analysis to unravel deep

79 magnetic sources. We then use these key elements to pinpoint a few outstanding questions that will guide
80 future research.
81
82 **2. Magnetization in the mantle**
83 Previous investigations on xenoliths and exposed sections of the mantle and lower crust[26-28] had
84 concluded that magnetite was primarily absent from the mantle and that, even if present, the conditions
85 would be too hot for it to carry a permanent magnetization. Wasilewski and co-workers referred to the
86 crust-mantle boundary as the Moho which fundamentally is a seismological boundary[1]. In this review, we
87 discuss magnetization with respect to the crust – mantle boundary. We acknowledge that, regardless of
88 the specific model used to approximate the depth of this boundary, uncertainties remain by the very
89 nature of inversion methods, although their accuracy continuously improves.
90 These early views have influenced the interpretation of satellite magnetic data for the past four
91 decades. Yet an increasing number of studies, for example in Australia, the Réunion Island, or the South
92 American platform, show that the uppermost mantle is unambiguously magnetized[29-31]. Also, several
93 spectral studies of magnetization use windows that are too small to detect a deeper base of
94 magnetization[32-33], which leaves uncertainties in the above assumptions. Moreover, many researchers
95 have used magnetic anomaly data where long-wavelengths are contaminated by distortions in data created
96 during the process of compilation from a really small magnetic surveys[90]. Thus, there are uncertainties in
97 the derived basal depth of magnetization where the magnetic anomaly compilations are not pristine or not
98 specifically processed to retain all anomaly wavelengths, where studies do not use a really large windows
99 (or at least examine them to ensure that they are not needed in the region), or studies that do not examine

[1] Wasilewski and co-workers referred to the crust-mantle boundary as the Moho which fundamentally is a seismological boundary. In this review, we discuss magnetization with respect to the crust – mantle boundary. We acknowledge that, regardless of the specific model used to approximate the depth of this boundary, uncertainties remain[33] by the very nature of inversion methods, although their accuracy continuously improves.

the fractal nature of magnetization because the fractal nature of magnetization makes shallower the derived depths to different layers.

In this section, we first review the information provided particularly in the last ten years by mantle xenoliths. Then we discuss the recent results from laboratory experiments specifically on the stability of magnetically remanent phases. Finally, we consider the insights from satellite and aeromagnetic surveys.

2.1. The magnetic record of mantle xenoliths

Identification of magnetic remanence in mantle rocks[33-42] raises the possibility that deep-seated magnetic remanence is present on earth. Mantle magnetization can be investigated further by considering the origin of long-wavelength magnetic anomalies[2] in remote sensing data. Pioneer work on the identification of magnetic phases in the upper mantle focused on the oceanic mantle because it is more directly accessible than the continental mantle. Most of these studies ultimately recognized that sea water inevitably percolates through fracture zones in the uppermost mantle, which leads to serpentinization[37-40]. This process generally forms iron oxides, namely magnetite, whose occurrence is confirmed through rocks dredged from the oceanic fracture zones[38, 41], recovered from ocean-floor drilling[42], and more recent detailed vertical magnetic mapping of the oceanic crust and uppermost mantle[43-45]. Serpentinization is the main mechanism through which the oceanic mantle acquires a permanent magnetization.

Further work to characterize the magnetic properties of mantle materials subsequently focused on metamorphosed peridotites from the Central Alps, in Switzerland and Italy, and from Mt. Stuart in Washington, USA[35], or serpentinites from the Manitoba nickel belt[36]. However, these efforts were somewhat flawed because the materials selected were either altered[33] or not representative of mantle materials at mantle depth. An alternative source of information is provided by upper mantle xenoliths,

[2]The term long-wavelengh for magnetic anomalies is relattive and has changed meaning since 1970s because magnetic surveys surveys were confined to regions smaller than 200-300 km and no continent-wide compilations were available[77, 78]; wavelengths > 60 km). POGO and Magsat satellite magnetic anomaly models extended the wavelengths of magnetic surveys all the way to the truncated core magnetic field models (~3,000 km). We use a definition based on the smallest wavelengths globally detectable from modern satellite data, *i.e.,* > 400-500 km.

such as those from from Lanzarote Island[34], which are fragments brought up to the surface embedded in an igneous rock.

2.1.1 Mantle oxidation and formation of magnetic minerals

Based on the presence of native iron in xenoliths from the lower continental crust in the West African craton[50-51], researchers extrapolated the stabilityconditions of native iron based on fO_2 (oxygen fugacity) to depths of 95 km, *i.e.*, below the crust-mantle boundary. The origin of deep magnetic phases was, at the time of these investigations, intriguing and several studies explained the formation of new magnetic phases through recrystallization below the crust-mantle boundary[52-53]. A broader dataset of upper mantle to lower crust xenoliths suggesting that the transition from granulite- to eclogite-facies might push the base of magnetization below the crust-mantle boundary, due to reactions involving magnetic phases, was compiled[28]. Based on Mossbauer Fe^{3+}/Fe^{2+} ratios in mantle xenoliths, fO_2 high enough for magnetite stability below the crust-mantle boundary were proposed[54]. Moreover, a recent analyses of inclusions of ultra-high pressure garnets in diamonds demonstrated that, in subduction settings, relative oxygen fugacity increases with depth, at least down to the depth of the mantle transition zone[55], thus expanding the stability field of magnetite. Reports of the magnetic properties of upper mantle xenoliths have become more abundant[17, 56-60], acknowledging partial oxidation of iron phases in the upper mantle.

More recently, the initial hypothesis of a non-magnetic upper mantle has been revisited with a careful analysis of new suites of fresh mantle xenoliths from different tectonic settings[61]. The identification of a Verwey transition univocally fingerprints magnetite in cold settings, suggesting the upper mantle can be magnetic. A new database of magnetite identified in mantle xenoliths includes North America[19], Massif Central, and Hawai'i[20, 62] and the North China Craton[63]. This empirical work led to further petrologic and magnetic models of oxidation of iron under mantle conditions[62]. Additionally, investigations have recently proven that oxidation of natural olivine is also plausible when mantle xenoliths ascend through the lithosphere under oxidizing conditions[64], extending an experimental result already reported for synthetic olivine samples[65].

148

149 2.1.2 Primary and secondary magnetisation in mantle xenoliths

150 Kimberlitic pipes and alkali basalt volcanoes naturally bring samples of mantle materials in the form
151 of xenoliths to the Earth's surface from great depths[46-47], possibly as deep as 400 km[16]. The ascent of
152 these xenoliths is extremely rapid, up to 90 km/h[48-49], which does not allow for significant alteration or
153 phase changes, hence their geochemical and petrological properties are considered representative of in-
154 situ compositions at depth, including potential magnetic carriers. Several pitfalls that need to be avoided
155 to measure the true magnetization of mantle xenoliths are outlined below. Some samples may undergo
156 alteration during and after their ascent. For example, inclusions of iron oxides, such as magnetite and
157 ilmenite, may form in iron-bearing silicates at mantle depth[66], during ascent, or through metasomatism
158 and crack healing[67-70]. Also, contamination by the host basalt occurs commonly by percolation along grain
159 boundaries during dilation related to ascent-decompression. Ultimately, supergene alteration may form
160 serpentine or hematite along grain boundaries. Any of these processes would substantially modify the
161 original and in-situ magnetic properties of mantle materials. For example, many previously analyzed
162 xenoliths[26] included materials marred by such contaminations and resulted in attributing a magnetization
163 that did not correspond to the upper mantle.

164 In contrast, more recently analyzed xenoliths[19-20, 61] from different regions of the world were fresh,
165 unaltered and free of such contaminations (Figure 2). The following criteria assist in the identification of
166 fresh material. First, when the Alt-S% index[71] <10%, this constitutes proof of a low degree of alteration in
167 primary sulfides. Second, when the loss-on-ignition (LOI) is less than 1%, this indicates of a low degree
168 of serpentinization[61]. Finally, a single thermal remanent magnetization (TRM) component in thermal
169 demagnetization experiments[20] shows the lack of chemical remanent magnetization or alteration. When
170 all these criteria are concurrently met, then the natural magnetic remanence (NRM) provided by mantle
171 xenoliths reflects the magnetic properties at the exposure level from which magnetic properties at depth
172 can be extrapolated.

Yet, the NRM measured in the laboratory at 1 atmosphere is different from magnetic remanence at a higher temperature and greater depths for three main reasons. First, the Curie temperature of pure magnetite increases with pressure/depth[72-73], such that, for example, Curie temperature for magnetite is ~600ºC at 1 GPa. Second, magnetic remanence increases with pressure[21, 74]; and finally the integrated magnetic remanence of a large volume peridotitic source at depth is likely weaker than that of the measured 1 cm^3 in the laboratory[75].

All existing magnetic studies of spinel-facies peridotite xenoliths concur that stoichiometric, pure magnetite, is the dominant magnetic phase, in unaltered mantle peridotites (for depths 30 to 80 km), with concentrations ranging from a few ppm to a maximum of ~3,500 ppm in the Bearpaw Mountains from the hydrated Farallon Plate[19]. Native iron, iron-nickel alloys (*e.g.,* josephinite, awaruite, and wairuite) and sulfides, when detected, are only present in trace amounts and do not carry a significant portion of the magnetic remanence, primarily because magnetite is quasi-ubiquitous in upper mantle xenoliths and dominates the NRM. Very few magnetic studies included garnet-facies peridotite xenoliths[26] and further investigations may reveal additional magnetically remanent phases.

Figure 2 shows the room-temperature variations of NRM as a function of low-field magnetic susceptibility (K_{lf}) in a collection of mantle xenoliths from distinct tectonic settings. This representation, known as Könisberger plot compares induced magnetization and remanent magnetization and pinpoints the material's thermoremanent magnetization acquired upon cooling and ascent. Overall K_{lf} remains bound within a narrow range of values around 500.10^{-6} [SI] regardless of tectonic setting. These values indicate that bulk magnetic susceptibility in fresh mantle rocks is primarily controlled by the paramagnetic ferromagnesian mineral assemblage (olivine, orthopyroxene, and clinopyroxene). The petrological composition of mantle rocks is homogeneous at a large scale, ranging from harzburgite to lherzolite. The primary NRM (TRM) reflects the abundance of magnetite and seems correlated with the tectonic setting: island arc xenoliths are less magnetic than those coming from continental rifted and cratonic areas. Yet xenoliths from hydrated deep mantle regions, such as the Bearpaw Mountains in Montana[76], exhibit a unique signature characterized by relatively high Koenigsberger ratios, indicative of

199 potential contributions to long-wavelength[#1] anomalies[19]. These xenoliths bear antigorite, a serpentine
200 phase indicative of hydration at temperatures around 600 ºC. Their hydration is attributed to the shallow
201 subduction of the Farallon Plate[76]. Those magnetite grains lay in a Day-Dunlop plot[147] very close to the
202 ideal SD state[19-20, 61] indicative of potential contributions to long-wavelength nomalies. Moreover, SD
203 particles are the most effective TRM intensity recorders[11] that can be one order of magnitude higher than
204 PSD grains.
205
206
207 **2.2. Insights from laboratory experiments**
208 In addition to studies of natural samples, presented in the previous section, high-pressure experiments
209 also support their importance as a deep source of magnetic remanence. Iron oxides, although
210 volumetrically minor phases in crustal and mantle rocks, are the most relevant magnetic phases in the
211 mantle owing to their high Curie or Néel temperatures[79]. Recent studies of natural samples and high-
212 pressure experiments both support their importance as a deep source of magnetic remanence.
213 However, data pertaining to the magnetic properties of minerals under mantle conditions are still
214 scant and the available information is only extrapolated from experimental data at lower pressure-
215 temperature (Supplementary Table S1). In the 2000s, Gilder and co-workers developed a novel approach
216 employing diamond anvil cells coupled with a superconducting quantum interference device (SQUID)
217 magnetometer to directly measure the magnetization vector of minerals under pressures exceeding 5
218 GPa[80]. Studies on the titanomagnetite solid-solution ($Fe_{3-x}Ti_xO_4$) series show a 2.8 fold increase of the
219 saturation remanent magnetization and magnetic coercivity of multidomain magnetite as a function of
220 increasing pressure[21-22, 80]. We acknowledge that the magnetic saturation generally decreases as
221 temperature increases but overall remains relatively high until the Curie / Néel temperature is reached.
222 Similar observations on SD magnetite indicate a marked increase in remanent coercivity and saturation
223 remanent magnetization between 1 and 3 GPa, corresponding to depths of ~30 to 90 km (op. cit.). The

variations of magnetic properties as a function of titanium content are not relevant in mantle rocks because magnetite in these rocks contains virtually no titanium.

The strong remanences and high coercivities shown by natural and synthetic samples under pressure (Supplementary Table S1), together with the steep increase of the Curie temperature by ~20 °C/GPa[72-73] (Figure 3) that can be increased to 600ºC at 1 GPa, also supports the role of magnetite as a deep source of magnetization in cold settings as inferred from the natural records[61].

However, magnetite is not stable below ~300 km depth (Figure 3) where it decomposes in equal molar fractions of hematite, α-Fe_2O_3, and Fe_4O_5[81] (Figure 3c) that could only recombine to form a high-pressure Fe_3O_4 phase below 600 km depth[82]. The Néel temperatures of hematite and the Fe_4O_5 phase have been recently investigated to mantle P-T conditions (Figure 3). The Néel temperature of Fe_4O_5 falls slightly above room temperature at ambient pressure[83] and does not increase significantly with pressure to play a role in mantle magnetism (Vasiukov et al., pers. comm., 2019). Hematite, on the other hand, retains its long-range magnetic order to temperatures in excess of 900 °C at 20 GPa, ~600 km depth[23], and it could likely be responsible for long-wavelength magnetic anomalies as discussed below.

Ultimately, these results highlight that the magnetic properties of minerals at depths relevant to the upper mantle (670 – 30 km) need further systematic investigations to fully evaluate their contributions to long-wavelength magnetic anomalies.

2.3 Remote detection of deep-seated magnetization

Identification of magnetic phases in mantle rocks raises the possibility that deep-seated magnetization is present on Earth. Mantle magnetization can be investigated further by analyzing magnetic anomaly data[9]. Amplitudes of the magnetic anomaly field arranged according to their wavelength (commonly known in the discipline as the Fourier amplitude spectrum) and specifically, slopes of the amplitude spectrum curve are theoretically related to depths of magnetic sources[24]. The determination of depth and depth extent of magnetic sources applies this concept[84-87]; the longer the wavelengths available to

construct the spectrum, the deeper one can sense (wavelengths needed are approximately 10 times the expected depth extent[88]. However, until this century, no accurate magnetic anomaly maps existed of large continental-scale regions, which are usually compiled from data collected over smaller areas at different times. Merging of neighboring smaller surveys was performed with ad-hoc data merging techniques to make their appearance seamless and, thus wavelengths between 100 and 500 km in these compilations, the most critical part of the wavelengths for probing depths below the middle of the continental crust were corrupted[89].

At the turn of the 20th century, methodologies of magnetic field data processing were developed[90] to ensure retention of long-wavelengths in the near-surface magnetic anomaly datasets. These included the use of temporally continuous core field models that attempt to model simultaneously all long-wavelength magnetic fields observed in the near-Earth environment (i.e., the core, crustal, ionospheric, and magnetospheric magnetic fields) using data from geomagnetic observatories and near-Earth magnetic field satellites such as POGO, Magsat, CHAMP, and Swarm (these models are called "the Comprehensive Models" of the magnetic field)[91]. The common approach in deriving magnetic anomaly maps has been the remove a five year period IGRF (International Geomagnetic Reference Field) core field models which have evolved over time to include shorter wavelength core derived magnetic fields. The magnetic field data collected over the years and processed with their respective five year period IGRFs do not merge well and they have to be modified at the individual small survey boundaries (the process called "stitching") in order to make compilations over larger regions. The process of stitching modifies the wavelength content of the resulting map[90] and any analysis of these maps introduces errors in its interpretation. One of the first continental-scale databases that included practically all wavelengths of the magnetic field "anomalies" from lithospheric sources was compiled for North America in the first decade of the 21st century[92] and now makes it possible to probe the continental mantle through spectral analysis of magnetic surveys. Australia is another continent-scale example where robust magnetic field anomalies of all wavelengths from lithospheric magnetic sources are available due to its Australia-Wide Airborne Geophysical Surveys magnetic anomaly survey backbone[93-94].

Comentado [MG1]: Can we expand a bit on what these methodologies are?

In the meantime, the spectral methods for probing deep magnetizations also needed to mature. Although the initial spectral depth determination techniques were developed in the 1960s and 1970s, it took considerable efforts to bring them to their present state. Like many natural phenomena, lithospheric magnetization is also found to be fractal in its distribution[95-100] and not necessarily made up of a collection of sources of uniform magnetization or having overall random distribution as has been previously considered[84-87]. This difference is important for the depths derived from the spectral depth determination techniques because the fractal (known also as having a "power-law") nature of magnetization intrinsically increases the slopes of magnetic anomaly spectra from which the depths are derived. Not considering (or not removing) fractalness of magnetization consistently increases the derived depths to magnetic layers and, thus, it makes the results of studies conducted without the cognizance of the fractal (or power-law) relationship inconclusive for determining whether the magnetization lies in the mantle. Depths from amplitude spectra can be estimated after making "correction" for the power-law behavior of the magnetic field spectra. The term coined for the removal of power-law or fractal characteristics from spectra is "de-fractaling".

Currently used spectral magnetic depth determination approaches for regional studies that take into account the power-law nature of magnetization use a number of related methodologies including directly using slopes of de-fractaled amplitude spectra[102]; matching observed magnetic spectra with spectra computed from layers of fractal magnetization[29, 101-104]; matching the peak in the magnetic spectra formed by the base of magnetization in the very long-wavelength part of the spectrum, when the peak exists from satisfying the random magnetization condition[90, 105-106] and a method specifically called the de-fractal method[107-108] which uses concurrently the methods of deriving depths from the slopes of de-fractaled amplitude spectra and matching the peak of the de-fractaled magnetic spectra. One of its advantages, that the other fractal parameter-based methods lack, is that it also can estimate the fractal parameter of the magnetic field. Its disadvantages are that it requires larger areas to construct reliably the low-wavenumber part of the amplitude spectra and it is currently not implemented automatically. The theoretical model study and real data examples of its implementation are discussed below.

Verification of the estimated fractal parameter is an integral part of the de-fractal method, where the derived fractal parameter is validated by the consistency of depth estimates from the first method discussed above[102]. On the other hand, the large uncertainty in the base of magnetization estimates is present when the fractal parameter (the parameter that governs the spatial characteristics of magnetization) cannot be estimated correctly[101], which hampers the accuracy of depth estimates from the first two methods above. Interestingly, the fractal parameter of the field can be estimated also by the slope of the log-log spectra. Even though the quality of this direct estimate depends on the noise in the spectra, it does provide an approximate cross-check on the fractal parameter derived from the de-fractal method.

The advantage of the de-fractal method is that it allows one to determine estimates of the base of magnetization over geologically meaningful regions. A simulation for a 40 km-thick magnetic crust and a fractal parameter $\alpha = 2$ for the magnetic field is given in Figure 4a. A practical example of spectral depth determination is given for the depth to the base of magnetization estimates in the cold Archean Superior province in eastern Canada (Figure 4c). Using previously published data[109-110]the de-fractal method suggests that the base of magnetization ranges between 60 and 95 km, based on several estimates in the region, offset by a few tens of kilometers and thus not representing lateral variation. The region has low surface heat flow (30-40 mW/m^2, [111]), the crust-mantle boundary depth is 30-35 km[112], and the upper mantle temperature estimates, based on S-wave tomography, range from 250°C just below the crust-mantle boundary to ~650°C at 80 km depth[113]. Thus, even with the shallowest base of magnetization estimates, these results show that the mantle does contribute to magnetic anomalies.

Recently, a spherical coordinate expression of magnetic anomaly spectra, taking into account the thickness of a magnetic layer and its magnetization and fractal parameter, was proposed[114]. However, because the unknown parameters are dependent on one another, they resorted to fixing the fractal parameter *a priori*, a previously chosen approach[104], which does not take into account the variation of the fractal parameter from region to region and can affect the estimates of depth of magnetization. Of interest to mantle magnetization, in a previous model for the regions of high quality[114], eastern North

America (east of 90°W) is the only continental region where the magnetic thickness is substantially greater than the Moho depth. One limitation of their present model is that the magnetic thickness and magnetization at each location is an average of data in 30° of a spherical cap (> 3000 km diameter). Thus, the actual variations related to most geologic and tectonic provinces are smeared out and subdued. In Australia, another region of high-quality continent-scale magnetic anomaly data, because of the > 3000 km large window of their study[114], the only estimates in central Australia covers largely the continental region. Other non-central estimates over Australia reflect combined results from continental and oceanic regions, where the magnetic thickness of the latter is generally much lower than its continental counterpart. Consequently, this averaging results in an extremely smooth variation of their magnetic thickness map with bias towards shallow values and thus these estimates[114] are unable to shed light on the issue of mantle magnetization.

On the other hand, in the Archean Yilgarn and Gawler cratons, studies that consider appropriate data widths, stabilization of long-wavelength spectral estimates, and fractal magnetization have yielded depths to the base of magnetization of 60-70 km[29] and are unambiguously in the mantle[115-116].

In general, spectral methods are of limited use in investigating magnetization in most subducting slabs because to ascertain magnetization at the depths of 50 to 100 km, one requires wavelengths of > 500 km to 1000 km, and this is much larger than the widths of the magnetic features atop subduction zones (which are less than 150 km). Here, forward modeling is most helpful in ascribing the sources and depths of magnetization, especially where geometries are better constrained and temperature models exist[24, 117].

In the last 50 years, since pioneer works[84], there have been a large number of studies that use spectral depth estimates without appropriately large windows, without sufficient model validation, without considering fractal nature of magnetization, and assumptions of fractal parameters. Many of these results may be quite useful for making geological inferences (as every segment of the amplitude spectrum implies depth to some magnetic subsurface horizon); however, because of the above limitations, they are

not able to definitively inform us about the magnetic nature of the uppermost mantle in regions where temperatures are sufficiently cold for its existence.

3. Location of the magnetized mantle?

Spectral analysis, laboratory experiments, and xenolith data is starting to show that magnetisation can exist in the mantle when it is relatively cold and hydrated or oxidized. Multiple studies[26, 125] reported trace volumes of magnetite in mantle xenoliths from continental cratonic and non-cratonic settings, as well as in the oceanic setting of Hawai'i. Yet these studies interpreted iron oxides supposedly at paramagnetic state formed in the late cooling of a non-depleted mantle as opposed to a primary phase[26]. Overall, the upper mantle should be expected to be magnetized in cold geothermal settings where the Curie depth would be below the crust-mantle boundary. Such settings include primarily cratons and subduction zones. This prediction is currently supported by remote spectral detection from magnetic anomalies[29].

Whilst, the strongest magnetic anomalies in the subduction setting are generally related to the crust of fossil or active volcanic arcs[118-119], a few studies have suggested that significant lateral magnetization contrast may be associated with the relatively cold subducting slabs[120]. The slabs deflect the Curie depth isotherm downwards from the comparatively warmer lithospheric mantle[117, 121]. Such colder regions are where the most prominent and deepest long-wavelength magnetic anomalies have been reported to date from aeromagnetic and satellite surveys[24, 29, 122-123].

An important source of mantle magnetization in the subduction regime is also the serpentinized mantle wedge between the subducting slab and the overriding lithosphere[24]. Because serpentinization reduces the density of the peridotitic mantle significantly, the telltale sign of serpentinized units is a low Bouguer gravity anomaly corresponding to the magnetic anomaly high which is observed over several subduction zones[24, 124].

Subduction settings also provide the most favorable geochemical-geodynamical context for the enrichment in iron oxides beyond crustal and mantle averages. The rapid subduction of oceanic slabs has two effects on the overriding mantle: in some cases, it introduces large volumes of magnetite-rich,

serpentinized oceanic peridotites deep in the subduction zone[126]; and it also transports large quantities of ferric iron, from the hydrothermally altered and/or serpentinized oceanic crust, into the mantle wedge region[127], hence a shift in fO_2 that promotes magnetite and/or hematite formation. These oxides can eventually reach the core-mantle boundary[128] due to their stability along subduction paths[129]). The potential sources of magnetic anomalies may, however, vary with depth, encompassing changes in the magnetic mineralogy in the slab.

Figure 3 compares the Curie and Néel temperatures in the Fe_3O_4-system with computed temperatures of the core of cold (*e.g.,* Solomon), hot (*e.g.,* North Lesser Antilles), and very hot (*e.g.,* South Chile) of subducting slabs to assess their role as deep mantle sources. While the Néel temperature of Fe_4O_5 is too low to sustain magnetic order at mantle depth even in cold settings, hematite remains magnetic at the depth of the mantle transition zone (670 km) along cold and possibly some of the moderately hot subduction geotherms[23]. The vast majority of these slabs are located in the Western Pacific region, suggesting that this region should be ferromagnetically very distinct from its surroundings. The strength of magnetic anomalies from deep sources in the subduction setting might be enhanced further by the piling of slab material associated with slab stagnation in the transition zone[130].

The presence of a frame of hematite-bearing magnetized rock in cold slabs at transition zone depths has far-reaching implications for the interpretation of the paleomagnetic records[23]. The strength of the remanent magnetization of hematite and its concentration in the subducted rocks will determine its contribution to magnetic anomalies observed on the surface of the planet. Hematite acquires near saturation remanent magnetization in weak fields that amounts to ~ 0.5 [$(A \times m^2)/kg$] at ambient conditions. Therefore, the remanent magnetization of hematite is 10-15 times stronger than the induced magnetization of magnetite of equal mass, and decreases very moderately with temperature (only by ~10% at temperatures 100 K below the critical temperature[79]. Nevertheless, as discussed in section 2.3., sources at 600 km depth will be difficult to detect due their small width and very small amplitudes at the Earth's surface.

The current knowledge on the Curie and Néel temperatures in iron oxides places the magnetic boundary in subducting slabs at approximately 600 km: the high-pressure Fe_3O_4 phase, stable at lower mantle conditions has temperatures of magnetic ordering below 227ºC in the 20-40 GPa pressure range[132] and decreases even further at higher pressures. However, the search for even deeper magnetic sources is far from being closed. For instance, at room temperature, the high-pressure phase of wüstite (FeO) is magnetic at pressures down to the base of the lower mantle[134], although the Curie or Néel temperatures of this phase at such high pressures are unknown. Moreover, a series of previously unknown iron oxides, stable at deep mantle conditions, have been discovered over the last decade[129, 135-140]. Some of these phases are stable down to the core-mantle boundary conditions but investigations of their Curie/Néel temperatures and other magnetic properties are still awaited.

4. Summary and Future Perspective

The old paradigm of a non-magnetic mantle has been challenged from several independent perspectives. New experimental data now shows the expanded stability of iron oxides to great depths (at least down to 670 km). Recent measurements on very fresh mantle xenoliths show that they systematically contain magnetite. New spectral methods to analyze magnetic anomaly data shows that crustal only sources cannot account for satellite observations. In addition to these advances, with the availability of new satellite data, such as the field gradients from future lower altitudes from the Swarm Mission, come new opportunities to evaluate the possible existence of deep sources of long-wavelength magnetic anomalies within the Earth's interior because these data can constrain the long-wavelengths necessary to derive estimates to the base of magnetization.

Clearly, these anomalies, previously thought to originate primarily from the Earth's crust[109, 141-143] most likely have mantle origins. Further, new experiments show that the remanence of iron oxides significantly increases with pressure[23]. These advances, combined with the revision of the nature of magnetic sources in the mantle through xenoliths rapidly brought to the surface of the Earth[19-20, 61-62] indicate that the mantle could contribute to magnetic anomalies, contrary to previous views held since

1979. The extent of these deep contributions would be, however, limited to specific regions of relatively cold temperatures (ancient cratons and subducting slabs) and to areas where the upper mantle has been substantially hydrated (Figure 5)[19, 24, 76].

The actual contributions from the upper mantle to magnetic anomalies can be quantified through further analysis of satellite magnetic data using modern methods such as de-fractal spectral analysis. Priority should be given to investigations in promising, low-geotherm regions, such as cratonic, subduction zones and old (>100 Ma) oceanic plates. Advanced studies focusing on the high pressure-high temperature magnetic properties of iron-bearing phases including iron oxides are also necessary to advance our understanding of deep magnetic sources in the Earth's interior. The already existing collections of deep mantle xenoliths, including lherzolites equilibrated in the garnet facies (eclogites), majorite-bearing and Ni-Fe alloy-bearing specimens, and possibly any wadsleyite-bearing specimens would also contribute to the validation of experimental studies. Finally, significant advances in our understanding of magnetic sources in the upper mantle, may also arise from new ab-initio calculations of magnetic properties of main ferromagnetic phases under high temperature and high pressure.

References:

[1] Aki, K., and Richards, P. G., 2002, Quantitative Seismology, 2nd Ed.

[2] Kono, M., 2009, Treatise on Geophysics, Volume 5: Geomagnetism, Elsevier Science.

[3] Pail, R., Bruinsma, S., Migliaccio, F., Förste, C., Goiginger, H., Schuh, W.-D., Höck, E., Reguzzoni, M., Brockmann, J. M., Abrikosov, O., Veicherts, M., Fecher, T., Mayrhofer, R., Krasbutter, I., Sansò, F., and Tscherning, C. C., 2011, First GOCE gravity field models derived by three different approaches: Journal of Geodesy, v. 85, no. 11, p. 819.

[4] Stechschulte, V. C., 1932, The Japanese earthquake of March 29, 1928, and the problem of depth of focus: Bulletin of the Seismological Society of America, v. 22, no. 2, p. 81-137.

[5] Bercovici, D., and Karato, S., 2003, Whole-mantle convection and the transition-zone water filter: Nature, v. 425, no. 6953, p. 39-44.

[6] Vine, F. J., and Matthews, D. H., 1963, Magnetic Anomalies Over Oceanic Ridges: Nature, v. 199, no. 4897, p. 947-949.

[7] Bloxham, J., 2000, Sensitivity of the geomagnetic axial dipole to thermal core–mantle interactions: Nature, v. 405, no. 6782, p. 63-65.

[8] Merrill, R. T., and McFadden, P. L., 2003, The geomagnetic axial dipole field assumption: Physics of the Earth and Planetary Interiors, v. 139, no. 3, p. 171-185.

[9] Finlay, C. C., Maus, S., Beggan, C. D., Bondar, T. N., Chambodut, A., Chernova, T. A., Chulliat, A., Golovkov, V. P., Hamilton, B., Hamoudi, M., Holme, R., Hulot, G., Kuang, W., Langlais, B., Lesur, V., Lowes, F. J., Lühr, H., Macmillan, S., Mandea, M., McLean, S., Manoj, C., Menvielle, M., Michaelis, I., Olsen, N., Rauberg, J., Rother, M., Sabaka, T. J., Tangborn, A., Tøffner-Clausen, L., Thébault, E., Thomson, A. W. P., Wardinski, I., Wei, Z., and Zvereva, T. I., 2010, International Geomagnetic Reference Field: the eleventh generation: Geophysical Journal International, v. 183, no. 3, p. 1216-1230. Lesur, V., Hamoudi, M., Choi, Y. et al. 2016, Building the second version of the World Digital Magnetic Anomaly Map (WDMAM). Earth Planet Sp 68, 27 (2016). doi.org/10.1186/s40623-016-0404-6.

[10] Butler, R. F., 1992, Paleomagnetism, Oxford, Blackwell Scientific Publications.

[11] Tauxe, L., 2006, Paleomagnetic principles and practice, Springer Science & Business Media.

[12] Katsura, T., Yoneda, A., Yamazaki, D., Yoshino, T., and Ito, E., 2010, Adiabatic temperature profile in the mantle: Physics of the Earth and Planetary Interiors, v. 183, no. 1, p. 212-218.

[13] Nagata, T., 1961, Rock magnetism, Tokyo, Maruzen Cy. Ltd.

[14] O'Reilly, W., 1984, Rock and mineral magnetism, New York, Blackie and Son Limited.

[15] Tauxe, L., 1998, Paleomagnetic principles and practice, Dordrecht, Kluwer Academic Publishers, Modern approaches in Geophysics.

[16] Haggerty, S. E., and Sautter, V., 1990, Ultradeep (Greater than 300 kilometers), ultramafic upper mantle xenoliths: Science, v. 248, no. 4958, p. 993-996.

[17] Abu-Aljarayesh, I., Mahmood, S., and Nasir, S., 1993, Magnetic study on lower crustal and upper mantle xenoliths from northeast Jordan: Abhath Al-Yarmouk. Pure Science and Engineering, v. 2, p. 41-54.

[18] Collerson, K. D., Hapugoda, S., Kamber, B. S., and Williams, Q., 2000, Rocks from the mantle transition zone: majorite-bearing xenoliths from Malaita, Southwest Pacific: Science, v. 288, no. 5469, p. 1215-1223.

[19] Friedman, S.A., Feinberg, J.M., Ferré, E.C., Demory, F., Martín-Hernández, F., Conder, J.A., and Rochette, P., 2014, Craton vs. rift uppermost mantle contributions to magnetic anomalies in the United States interior: Tectonophysics, v. 624-625, p. 15-23.

[20] Martín-Hernández, F., Ferré, E. C., and Friedman, S. A., 2014, Remanent magnetization in fresh xenoliths derived from combined demagnetization experiments: Magnetic mineralogy, origin and implications for mantle sources of magnetic anomalies: Tectonophysics, v. 624-625, p. 24-31.

[21] Gilder, S. A., LeGoff, M., Chervin, J.-C., and Peyronneau, J., 2004, Magnetic properties of single and multi-domain magnetite under pressures from 0 to 6 GPa: Geophys. Res. Lett., v. 31, L10612, doi:10.1029/2004GL019844.

[22] Gilder, S. A., and Le Goff, M., 2008, Systematic pressure enhancement of titanomagnetite magnetization: Geophys. Res. Lett., v. 35, L10302, doi:10.1029/2008GL033325.

[23] Kupenko, I., Aprilis, G., Vasiukov, D. M., McCammon, C., Chariton, S., Cerantola, V., Kantor, I., Chumakov, A. I., Rüffer, R., Dubrovinsky, L., and Sanchez-Valle, C., 2019, Magnetism in cold subducting slabs at mantle transition zone depths: Nature, v. 570, no. 7759, p. 102-106. Klotz, S., Strässle, T. & Hansen, T. 2013, Pressure dependence of Morin transition in α-Fe_2O_3 hematite. Europhys. Lett. 104, 16001.

[24] Blakely, R. J., Brocher, T. M., and Wells, R. E., 2005, Subduction-zone magnetic anomalies and implications for hydrated forearc mantle: Geology, v. 33, no. 6, p. 445-448.

[25] Bilim, F., Akay, T., Aydemir, A., and Kosaroglu, S., 2016, Curie point depth, heat-flow and radiogenic heat production deduced from the spectral analysis of the aeromagnetic data for

geothermal investigation on the Menderes Massif and the Aegean Region, western Turkey: Geothermics, v. 60, p. 44-57.

[26] Wasilewski, P. J., Thomas, H. H., and Mayhew, M. A., 1979, The Moho as a magnetic boundary: Geophysical Research Letters, v. 6, p. 541-544.

[27] Shive, P. N., 1990, The Ivrea Zone and lower crustal magnetization: Tectonophysics, v. 182, no. 1, p. 161-167.

[28] Wasilewski, P. J., and Mayhew, M. A., 1992, The Moho as a magnetic boundary revisited: Geophysical Research Letters, v. 19, no. 22, p. 2259-2262.

[29] Chopping, R., and Kennett, B. L. N., 2015, Maximum depth of magnetisation of Australia, its uncertainty, and implications for Curie depth: GeoResJ, v. 7, p. 70-77.

[30] Gailler, L.-S., Lénat, J.-F., and Blakely, R. J., 2016, Depth to Curie temperature or bottom of the magnetic sources in the volcanic zone of la Réunion hot spot: Journal of Volcanology and Geothermal Research, v. 324, p. 169-178.

[31] Idárraga-García, J., and Vargas, C. A., 2018, Depth to the bottom of magnetic layer in South America and its relationship to Curie isotherm, Moho depth and seismicity behavior: Geodesy and Geodynamics, v. 9, no. 1, p. 93-107.

[32] Wang, J., and Li, C.-F., 2015, Crustal magmatism and lithospheric geothermal state of western North America and their implications for a magnetic mantle: Tectonophysics, v. 638, p. 112-125.

[33] van der Meijde, M., and Pail, R., 2020, Impact of uncertainties of GOCE gravity model on crustal thickness estimates: Geophysical Journal International, v. 221, no. 2, p. 1226-1231.

[34] Frisch, T., 1971, Alteration of chrome spinel in a dunite nodule from Lanzarote, Canary Islands: Lithos, v. 4, no. 1, p. 83-91.

[35] Evans, B. W., and Frost, B. R., 1975, Chrome-spine1 in progressive metamorphism—A preliminary analysis: Geochimica et Cosmochimica Acta, v. 39, p. 959-972.

[36] Bliss, N. W., and Maclean, W. H., 1976, The paragenesis of zoned chromite from central Manitoba, p. 973-990.

[37] Hess, H. H., 1962, History of Ocean Basins, in Engel, A. E. J., James, H. L., and Leonard, B. F., eds., Petrologic Studies: A Volume to Honor A.G. Buddington: Boulder, Geological Society of London, p. 599-620.

[38] Christensen, N. I., 1972, The Abundance of Serpentinites in the Oceanic Crust: The Journal of Geology, v. 80, no. 6, p. 709-719.

[39] Faccenda, M., Gerya, T. V., and Burlini, L., 2009, Deep slab hydration induced by bending-related variations in tectonic pressure: Nature Geoscience, v. 2, no. 11, p. 790-793.

[40] Abily, B., Ceuleneer, G., and Launeau, P., 2011, Synmagmatic normal faulting in the lower oceanic crust: Evidence from the Oman ophiolite: Geology, v. 39, no. 4, p. 391-394.

[41] Detrick, R. S., White, R. S., and Purdy, G. M., 1993, Crustal structure of North Atlantic Fracture Zones: Reviews of Geophysics, v. 31, no. 4, p. 439-458.

[42] Parkinson, C., 1998, Emplacement of the East Sulawesi Ophiolite: evidence from subophiolite metamorphic rocks: Journal of Asian Earth Sciences, v. 16, no. 1, p. 13-28.

[43] Arkani-Hamed, J., 1988, Remanent magnetization of the oceanic upper mantle: Geophys. Res. Lett., v. 15, no. 1, p.48-51.

[44] Tivey, M., Takeuchi, A., and Scientific Party, W., 1998, A submersible study of the western intersection of the Mid-Atlantic ridge and Kane fracture zone (WMARK): Marine Geophysical Researches, v. 20, no. 3, p. 195-218.

[45] Tominaga, M., Tivey, M. A., MacLeod, C. J., Morris, A., Lissenberg, C. J., Shillington, D. J., and Ferrini, V., 2016, Characterization of the in situ magnetic architecture of oceanic crust (Hess Deep) using near-source vector magnetic data: Journal of Geophysical Research: Solid Earth, v. 121, no. 6, p. 4130-4146.

[46] Nixon, P. H., 1987, Mantle xenoliths, Chichester, John Wiley & Sons.

[47] Carlson, R. W., 2007, The Mantle and Core, Elsevier, Treatise on Geochemistry.

[48] Demouchy, S., Jacobsen, S. D., Gaillard, F., and Stern, C. R., 2006, Rapid magma ascent recorded by water diffusion profiles in mantle olivine: Geology, v. 34, no. 6, p. 429-432.

[49] Peslier, A. H., Bizimis, M., and Matney, M., 2015, Water disequilibrium in olivines from Hawaiian peridotites: Recent metasomatism, H diffusion and magma ascent rates: Geochimica et Cosmochimica Acta, v. 154, p. 98-117.

[50] Haggerty, S. E., and Toft, P. B., 1985, Native iron in the continental lower crust: petrological and geophysical implications: Science, v. 229, no. 4714, p. 647-649.

[51] Toft, P. B., and Haggerty, S. E., 1988, Limiting depth of magnetization in cratonic lithosphere: Geophysical Research Letters, v. 15, no. 5, p. 530–533.

[52] Pechersky, D. M., and Genshaft, Y. S., 2001, Petromagnetism of the continental lithosphere and the origin of regional magnetic anomalies: A review: Russian Journal of Earth Sciences, v. 3, no. 2, p. 1-36.

[53] Pechersky, D. M., and Genshaft, Y. S., 2002, Petromagnetism of the continental crust: A summary of 20th century research: Phys. Solid Earth 38, 4–36., v. 38, p. 4-36.

[54] Canil, D., Virgo, D., and Scarfe, C. M., 1990, Oxidation state of mantle xenoliths from British Columbia, Canada: Contributions to Mineralogy and Petrology, v. 104, no. 4, p. 453-462.

[55] Kiseeva, E. S., Vasiukov, D. M., Wood, B. J., McCammon, C., Stachel, T., Bykov, M., Bykova, E., Chumakov, A., Cerantola, V., Harris, J. W., and Dubrovinsky, L., 2018, Oxidized iron in garnets from the mantle transition zone: Nature Geoscience, v. 11, no. 2, p. 144-147.

[56] Warner, R. D., and Wasilewski, P. J., 1995, Magnetic petrology of lower crust and upper mantle xenoliths from McMurdo Sound, Antarctica: Tectonophysics, v. 249, no. 1-2, p. 69-92.

[57] Warner, R. D., and Wasilewski, P. J., 1997, Magnetic petrology of arc xenoliths from Japan and Aleutian Islands: J. Geophys. Res., v. 102, no. B9, p. 20225-20243.

[58] Alva-Valdivia, L. M., Rosas-Elguera, J., Bravo-Medina, T., Urrutia-Fucugauchi, J., Henry, B., Caballero, C., Rivas-Sanchez, M. L., Goguitchaichvili, A., and Lopez-Loera, H., 2005, Paleomagnetic and magnetic fabric studies of the San Gaspar Ignimbrite, western Mexico - constraints on emplacement mode and source vents: Journal of Volcanology and Geothermal Research, v. 147, p. 68-80.

584 [59] Pearson, D. G., Canil, D., and Shirey, S. B., 2003, Mantle samples included in volcanic rocks:
585 xenoliths and diamonds, in Carlson, R. W., ed., Treatise on Geochemistry. Vol. 2. The Mantle and
586 Core, Elsevier, p. 171-276.
587 [60] Al-Malabeh, A., El-Hasan, T., and Lataifeh, M., 2009, Geochemical, petrographic and magnetic
588 characteristics of spinel lherzolite mantle xenoliths from Jabal Remah volcano, Jordan: American
589 Journal of Applied Sciences, v. 6, no. 7, p. 1308-1312.
590 [61] Ferré, E. C., Friedman, S. A., Martín-Hernández, F., Feinberg, J. M., Conder, J. A., and Ionov, D. A.,
591 2013, The magnetism of mantle xenoliths and potential implications for sub-Moho magnetic sources:
592 Geophysical Research Letters, 40, 105– 110, doi:10.1029/2012GL054100.
593 [62] Ferré, E. C., Friedman, S. A., Martin-Hernandez, F., Feinberg, J. M., Till, J. L., Ionov, D. A., and
594 Conder, J. A., 2014, Eight good reasons why the uppermost mantle could be magnetic:
595 Tectonophysics, v. 624-625, p. 3-14.
596 [63] Li, Z., Zheng, J., Zeng, Q., Liu, Q., and Griffin, W. L., 2014, Magnetic mineralogy of pyroxenite
597 xenoliths from Hannuoba basalts, northern North China Craton: Implications for magnetism in the
598 continental lower crust: Journal of Geophysical Research: Solid Earth, v. 119, no. 2, p. 806-821.
599 [64] Knafelc, J., Filiberto, J., Ferré E. C., Conder J.A., Costello, L., Crandall J.R., Dyar, M. D., Friedman
600 S.A., Hummer D.R., and Schwenzer, S.P., 2019, The effect of oxidation on the mineralogy and
601 magnetic properties of olivine, American Mineralogist, v. 104, p. 694-702.
602 [65] Brewster, D., and O'Reilly, W., 1988, Magnetic properties of synthetic analogues of the altered
603 olivines of igneous rocks: Geophysical Journal, v. 95, p. 421-432.
604 [66] Sen, G., and Jones, R. E., 1988, Exsolved silicate and oxide phases from clinopyroxenes in a single
605 Hawaiian xenolith: Implications for oxidation state of the Hawaiian upper mantle: Geology, v. 16, no.
606 1, p. 69-72.
607 [67] Drury, M. R., and van Roermund, H. L. M., 1988, Metasomatic origin for Fe-Ti-rich multiphase
608 inclusions in olivine from kimberlite xenoliths: Geology, v. 16, no. 11, p. 1035-1038.

609 [68] Drury, M. R., and van Roermund, H. L. M., 1989, Reply to comment by R.L. Hervig on
610 "Metasomatic origin for Fe-Ti-rich multiphase inclusions in olivine from kimberlite xenoliths":
611 Geology, v. 17, no. 7, p. 676-677.
612 [69] Hervig, R. L., 1989, Comment on "Metasomatic origin for Fe-Ti-rich multiphase inclusions in
613 olivine from kimberlite xenoliths": Geology, v. 17, no. 7, p. 675-676.
614 [70] Neal, C. R., Haggerty, S. E., and Sautter, V., 2001, "Majorite" and "Silicate Perovskite" Mineral
615 Compositions in Xenoliths from Malaita: Science, v. 292, no. 5519, p. 1015-1015.
616 [71] Alard, O., Lorand, J.-P., Reisberg, L., Bodinier, J. L., Dautria, J. M., and O'Reilly, S. Y., 2011,
617 Volatile-rich metasomatism in Montferrier xenoliths (Southern France): Implications for the
618 abundances of chalcophile and highly siderophile elements in the subcontinental mantle: Journal of
619 Petrology, v. 52, no. 10, p. 2009-2045.
620 [72] Samara, G. A., and Giardini, A. A., 1969, Effect of pressure on the Néel temperature of magnetite:
621 Physical Review, v. 186, no. 2, p. 577-580.
622 [73] Schult, A., 1970, Effect of pressure on the Curie temperature of titanomagnetites [(1 - x).Fe_3O_4 -
623 x.$TiFe_2O_4$]: Earth and Planetary Science Letters, v. 10, no. 1, p. 81-86.
624 [74] Volk, M. W. R., and Feinberg, J. M., 2019, Domain State and Temperature Dependence of Pressure
625 Remanent Magnetization in Synthetic Magnetite: Implications for Crustal Remagnetization:
626 Geochemistry, Geophysics, Geosystems, v. 20, no. 5, p. 2473-2483.
627 [75] Idoko, C. M., Conder, J. A., Ferré, E. C., and Filiberto, J., 2019, The potential contribution to long
628 wavelength magnetic anomalies from the lithospheric mantle: Physics of the Earth and Planetary
629 Interiors, v. 292, p. 21-28.
630 [76] Facer, J., Downes, H., and Beard, A., 2009, In situ Serpentinization and Hydrous Fluid
631 Metasomatism in Spinel Dunite Xenoliths from the Bearpaw Mountains, Montana, USA: Journal of
632 Petrology, v. 50, no. 8, p. 1443-1475.
633 [77] Hall, D. H., 1974, Long-wavelength aeromagnetic anomalies and deep crustal magnetization in
634 Manitoba and northwestern Ontario, Canada: Journal of Geophysics, v. 40, no. 1, p. 403-430.

635 [78] Krutikhovskaya, Z., and Pashkevich, I., 1979, Long-wavelength magnetic anomalies as a source of
636 information about deep crustal structure: Journal of Geophysics, v. 46, no. 1, p. 301-317.
637 [79] Dunlop, D. J., and Kletetschka, G., 2001, Multidomain hematite: A source of planetary magnetic
638 anomalies?: Geophysical Research Letters, v. 28, no. 17, p. 3345-3348.
639 [80] Gilder, S. A., and LeGoff, M., 2005, Pressure dependence on the magnetic properties of
640 titanomagnetite using the reversible susceptibility method, in Chen, J., Wang, Y., Duffy, T. S., Shen,
641 G., and Dobrzhinetskaya, L. F., eds., Advances in High-Pressure Technology for Geophysical
642 Applications: Amsterdam, Elsevier, p. 315-335.
643 [81] Woodland, A. B., Frost, D. J., Trots, D. M., Klimm, K., and Mezouar, M., 2012, In situ observation
644 of the breakdown of magnetite (Fe_3O_4) to Fe_4O_5 and hematite at high pressures and temperatures:
645 American Mineralogist, v. 97, no. 10, p. 1808-1811.
646 [82] Uenver-Thiele, L., Woodland, A. B., Seitz, H.-M., Downes, H., and Altherr, R., 2017, Metasomatic
647 Processes Revealed by Trace Element and Redox Signatures of the Lithospheric Mantle Beneath the
648 Massif Central, France: Journal of Petrology, v. 58, no. 3, p. 395-422.
649 [83] Ovsyannikov, S. V., Bykov, M., Bykova, E., Kozlenko, D. P., Tsirlin, A. A., Karkin, A. E.,
650 Shchennikov, V. V., Kichanov, S. E., Gou, H., Abakumov, A. M., Egoavil, R., Verbeeck, J.,
651 McCammon, C., Dyadkin, V., Chernyshov, D., van Smaalen, S., and Dubrovinsky, L. S., 2016,
652 Charge-ordering transition in iron oxide Fe_4O_5 involving competing dimer and trimer formation:
653 Nature Chemistry, v. 8, no. 5, p. 501-508.
654 [84] Spector, A., and Grant, F. S., 1970, Statistical models for interpreting aeromagnetic data:
655 Geophysics, v. 35, no. 2, p. 293-302.
656 [85] Bhattacharyya, B. K., and Leu, L.-K., 1975, Analysis of magnetic anomalies over Yellowstone
657 National Park: Mapping of Curie point isothermal surface for geothermal reconnaissance: Journal of
658 Geophysical Research (1896-1977), v. 80, no. 32, p. 4461-4465.
659 [86] Bhattacharyya, B. K., and Leu, L.,1977, Spectral analysis of gravity and magnetic anomalies due to
660 rectangular prismatic bodies: Geophysics, v. 42, no.1, p. 41-50.

661 [87] Okubo, Y., Graf, R. J., Hansen, R. O., Ogawa, K., and Tsu, H., 1985, Curie-point depths of the island
662 of Kyushu and surrounding areas, Japan: Geophysics, v. 50, no. 3, p. 481-494.
663 [88] Ravat, D., 2007, Crustal Magnetic Fields, In: Gubbins D., Herrero-Bervera E. (eds) Encyclopedia of
664 Geomagnetism and Paleomagnetism. Springer, Dordrecht, p. 140-144.
665 [89] Langel, R. A., and Hinze, W. J., 1998, The Magnetic Field of the Earth's Lithosphere: The Satellite
666 Perspective, Cambridge, Cambridge University Press.
667 [90] Ravat, D., Whaler, K. A., Pilkington, M., Sabaka, T., and Purucker, M., 2002, Compatibility of high-
668 altitude aeromagnetic and satellite-altitude magnetic anomalies over Canada: Geophysics, v. 67, no.
669 2, p. 546-554.
670 [91] Sabaka, T. J., Olsen, N., and Langel, R. A., 2002, A comprehensive model of the quiet-time, near-
671 Earth magnetic field: phase 3: Geophysical Journal International, v. 151, no. 1, p. 32-68.
672 [92] Ravat, D., Finn, C., Hill, P., Kucks, R., Phillips, J., Blakely, R., Bouligand, C., Sabaka, T., Elshayat,
673 A., Aref, A., and Elawadi, E., 2009, A Preliminary, Full Spectrum, Magnetic Anomaly Grid of the
674 United States with Improved Long Wavelengths for Studying Continental Dynamics: A Website for
675 Distribution of Data, USGS Open File Report, 2009-1258.
676 [93] Minty, B. R. S., Milligan, P. R., Luyendyk, T., and Mackey, T., 2003, Merging airborne magnetic
677 surveys into continental-scale compilations: Geophysics, v. 68, no. 3, p. 988-995.
678 [94] Milligan, P., Minty, B., Richardson, M., and Franklin, R., 2009, The australia-wide airborne
679 geophysical survey - accurate continental magnetic coverage: ASEG Extended Abstracts, v. 2009, no.
680 1, p. 1-9.
681 [95] Gregotski, M. E., Jensen, O., and Arkani-Hamed, J., 1991, Fractal stochastic modeling of
682 aeromagnetic data: Geophysics, v. 56, no. 11, p. 1706-1715.
683 [96] Pilkington, M., and Todoeschuck, J. P., 1993, Fractal magnetization of continental crust:
684 Geophysical Research Letters, v. 20, no. 7, p. 627-630.
685 [97] Maus, S., and Dimri, V. P., 1994, Scaling properties of potential fields due to scaling sources:
686 Geophysical Research Letters, v. 21, no. 10, p. 891-894.

687 [98] Maus, S., and Dimri, V., 1995, Potential field power spectrum inversion for scaling geology: Journal
688 of Geophysical Research: Solid Earth, v. 100, no. B7, p. 12605-12616.
689 [99] Maus, S., and Dimri, V., 1996, Depth estimation from the scaling power spectrum of potential
690 fields?: Geophysical Journal International, v. 124, no. 1, p. 113-120.
691 [100] Fedi, M., Quarta, T., and De Santis, A., 1997, Inherent power-law behavior of magnetic field power
692 spectra from a Spector and Grant ensemble: Geophysics, v. 62, no. 4, p. 1143-1150.
693 [101] Maus, S., Gordon, D., and Fairhead, D., 1997, Curie-temperature depth estimation using a self-
694 similar magnetization model: Geophysical Journal International, v. 129, no. 1, p. 163-168.
695 [102] Bansal, A., Gabriel, G., Dimri, V., and Krawczyk, C., 2011, Estimation of depth to the bottom of
696 magnetic sources by a modified centroid method for fractal distribution of sources: An application to
697 aeromagnetic data in Germany: Geophysics, v. 76, no. 3, p. L11-L22.
698 [103] Maus, S., Barckhausen, U., Berkenbosch, H., Bournas, N., Brozena, J., Childers, V., Dostaler, F.,
699 Fairhead, J. D., Finn, C., von Frese, R. R. B., Gaina, C., Golynsky, S., Kucks, R., Lühr, H., Milligan,
700 P., Mogren, S., Müller, R. D., Olesen, O., Pilkington, M., Saltus, R., Schreckenberger, B., Thébault,
701 E., and Caratori Tontini, F., 2009, EMAG2: A 2–arc min resolution Earth Magnetic Anomaly Grid
702 compiled from satellite, airborne, and marine magnetic measurements: Geochem. Geophys. Geosyst.,
703 10, Q08005, doi:10.1029/2009GC002471.
704 [104] Bouligand, C., Glen, J., Blakely, R., and Ravat, D., 2009, Estimating the depth-extent of crustal
705 magnetic sources from an improved aeromagnetic compilation of the western US.
706 [105] Blakely, R. J., 1988, Curie temperature isotherm analysis and tectonic implications of aeromagnetic
707 data from Nevada: Journal of Geophysical Research: Solid Earth, v. 93, no. B10, p. 11817-11832.
708 [106] Ross, H. E., Blakely, R. J., and Zoback, M. D., 2006, Testing the use of aeromagnetic data for the
709 determination of Curie depth in California: Geophysics, v. 71, no. 5, p. L51-L59.
710 [107] Salem, A., Green, C., Ravat, D., Singh, K. H., East, P., Fairhead, J. D., Mogren, S., and Biegert, E.,
711 2014, Depth to Curie temperature across the central Red Sea from magnetic data using the de-fractal
712 method: Tectonophysics, v. 624-625, p. 75-86.

[108] Ravat, D., Morgan, P., and Lowry, A. R., 2016, Geotherms from the temperature-depth–constrained solutions of 1-D steady-state heat-flow equation: Geosphere, v. 12, no. 4, p. 1187-1197.

[109] Dunlop, D. J., Özdemir, Ö., and Costanzo-Alvarez, V., 2010, Magnetic properties of rocks of the Kapuskasing uplift (Ontario, Canada) and origin of long-wavelength magnetic anomalies: Geophysical Journal International, v. 183, no. 2, p. 645-658.

[110] Pilkington, M., and Percival, J. A., 1999, Crustal magnetization and long-wavelength aeromagnetic anomalies of the Minto block, Quebec: Journal of Geophysical Research: Solid Earth, v. 104, no. B4, p. 7513-7526.

[111] Lévy, F., Jaupart, C., Mareschal, J. C., Bienfait, G., and Limare, A., 2010, Low heat flux and large variations of lithospheric thickness in the Canadian Shield: Journal of Geophysical Research: Solid Earth, v. 115, no. B6.

[112] Chulick, G. S., and Mooney, W. D., 2002, Seismic Structure of the Crust and Uppermost Mantle of North America and Adjacent Oceanic Basins: A Synthesis: Bulletin of the Seismological Society of America, v. 92, no. 6, p. 2478-2492.

[113] Shapiro, N. M., Ritzwoller, M. H., Mareschal, J. C., and Jaupart, C., 2004, Lithospheric structure of the Canadian Shield inferred from inversion of surface-wave dispersion with thermodynamic a priori constraints: Geological Society, London, Special Publications, v. 239, no. 1, p. 175-194.

[114] Vervelidou, F., and Thébault, E., 2015, Global maps of the magnetic thickness and magnetization of the Earth's lithosphere: Earth, Planets and Space, v. 67, no. 1, p. 173.

[115] Kennett, B. L. N., Salmon, M., Saygin, E., and Group, A. W., 2011, AusMoho: the variation of Moho depth in Australia: Geophysical Journal International, v. 187, no. 2, p. 946-958.

[116] Salmon, M., Kennett, B. L. N., Stern, T., and Aitken, A. R. A., 2013, The Moho in Australia and New Zealand: Tectonophysics, v. 609, p. 288-298.

[117] Arkani-Hamed, J., and Strangway, D. W., 1987, An interpretation of magnetic signatures of subduction zones detected by MAGSAT: Tectonophysics, v. 133, p. 45-55.

[118] Finn, C., 1994, Aeromagnetic evidence for a buried Early Cretaceous magmatic arc, northeast Japan: Journal of Geophysical Research: Solid Earth, v. 99, no. B11, p. 22165-22185.

[119] Campos-Enríquez, J. O., Espinosa-Cardeña, J. M., and Oksum, E., 2019, Subduction control on the curie isotherm around the Pacific-North America plate boundary in northwestern Mexico (Gulf of California). Preliminary results: Journal of Volcanology and Geothermal Research, v. 375, p. 1-17.

[120] Arkani-Hamed, J., and Strangway, D. W., 1985, Intermediate-scale magnetic anomalies of the Earth: Geophysics, v. 50, no. 12, p. 2817-2830.

[121] Clark, S. C., Frey, H., and Thomas, H. H., 1985, Satellite magnetic anomalies over subduction zones: the Aleutian Arc anomaly: Geophysical Research Letters, v. 12, no. 1, p. 41-44.

[122] Schlinger, C. M., 1985, Magnetization of lower crust and interpretation of regional magnetic anomalies: Example from Lofoten and Vesterålen, Norway: Journal of Geophysical Research: Solid Earth, v. 90, no. B13, p. 11484-11504.

[123] Williams, S. E., and Gubbins, D., 2019, Origin of Long-Wavelength Magnetic Anomalies at Subduction Zones: Journal of Geophysical Research: Solid Earth, v. 124, no. 9, p. 9457-9473.

[124] Saad, A. H., 1969, Magnetic properties of ultramafic rocks from Red Mountain, California: Geophysics, v. 34, p. 974-987.

[125] Wasilewski, P. J., 1987, Magnetic properties of mantle xenoliths and the magnetic character of the crust-mantle boundary, in Nixon, P. H., ed., Mantle Xenoliths: London, John Wiley and Sons Ltd., p. 577-588.

[126] Klein, F., Bach, W., Humphris, S. E., Kahl, W.-A., Jöns, N., Moskowitz, B., and Berquó, T. S., 2014, Magnetite in seafloor serpentinite—Some like it hot: Geology, v. 42, no. 2, p. 135-138.

[127] Lécuyer, C., and Ricard, Y., 1999, Long-term fluxes and budget of ferric iron: implication for the redox states of the Earth's mantle and atmosphere: Earth and Planetary Science Letters, v. 165, p. 197-211.

[128] Dobson, D. P., and Brodholt, J. P., 2005, Subducted banded iron formations as a source of ultralow-velocity zones at the core–mantle boundary: Nature, v. 434, no. 7031, p. 371-374.

764 [129] Bykova, E., Dubrovinsky, L., Dubrovinskaia, N., Bykov, M., McCammon, C., Ovsyannikov, S. V.,
765 Liermann, H. P., Kupenko, I., Chumakov, A. I., Rüffer, R., Hanfland, M., and Prakapenka, V., 2016,
766 Structural complexity of simple Fe_2O_3 at high pressures and temperatures: Nature Communications,
767 v. 7, no. 1, p. 10661.
768 [130] Fukao, Y., Obayashi, M., and Nakakuki, T., 2009, Stagnant Slab: A Review: Annual Review of
769 Earth and Planetary Sciences, v. 37, no. 1, p. 19-46.
770 [131] Gubbins, D., and Herrero-Bervera, E., 2007, Encyclopedia of Geomagnetism and Paleomagnetism,
771 Dordrecht, Springer, p. 250.
772 [132] Kozlenko, D. P., Dubrovinsky, L. S., Kichanov, S. E., Lukin, E. V., Cerantola, V., Chumakov, A.
773 I., and Savenko, B. N., 2019, Magnetic and electronic properties of magnetite across the high pressure
774 anomaly: Scientific Reports, v. 9, no. 1, p. 4464.
775 [133] Xu, W., Machavariani, G. Y., Rozenberg, G. K., and Pasternak, M., 2004, Mössbauer and
776 resistivity studies of the magnetic and electronic properties of the high-pressure phase of Fe_3O_4:
777 Physical Review B, v. 70, no. 17, p. 174106.
778 [134] Hamada, M., Kamada, S., Ohtani, E., Mitsui, T., Masuda, R., Sakamaki, T., Suzuki, N., Maeda, F.,
779 and Akasaka, M., 2016, Magnetic and spin transitions in wüstite: A synchrotron Mössbauer
780 spectroscopic study: Physical Review B, v. 93, no. 15, p. 155165.
781 [135] Hu, Q., Kim, D. Y., Liu, J., Meng, Y., Yang, L., Zhang, D., Mao, W. L., and Mao, H.-k., 2017,
782 Dehydrogenation of goethite in Earth's deep lower mantle: Proceedings of the National Academy of
783 Science, v. 114, p. 1498-1501.
784 [136] Ishii, T., Uenver-Thiele, L., Woodland, A. B., Alig, E., and Boffa Ballaran, T., 2018, Synthesis and
785 crystal structure of Mg-bearing Fe9O11: New insight in the complexity of Fe-Mg oxides at conditions
786 of the deep upper mantle: American Mineralogist, v. 103, no. 11, p. 1873-1876.
787 [137] Koemets, E., Fedotenko, T., Khandarkhaeva, S., Bykov, M., Bykova, E., Thielmann, M., Chariton,
788 S., Aprilis, G., Koemets, I., and Liermann, H.-P., 2019, FeOOH instability at the lower mantle
789 conditions: arXiv preprint arXiv:1908.02114.

790 [138] Lavina, B., Dera, P., Kim, E., Meng, Y., Downs, R. T., Weck, P. F., Sutton, S. R., and Zhao, Y.,
791 2011, Discovery of the recoverable high-pressure iron oxide Fe_4O_5: Proceedings of the National
792 Academy of Sciences, v. 108, no. 42, p. 17281-17285.
793 [139] Lavina, B., and Meng, Y., 2015, Unraveling the complexity of iron oxides at high pressure and
794 temperature: Synthesis of Fe_5O_6: Science Advances, v. 1, no. 5, p. e1400260.
795 [140] Sinmyo, R., Bykova, E., Ovsyannikov, S. V., McCammon, C., Kupenko, I., Ismailova, L., and
796 Dubrovinsky, L., 2016, Discovery of Fe_7O_9: a new iron oxide with a complex monoclinic structure:
797 Scientific Reports, v. 6, no. 1, p. 32852.
798 [141] Ouabego, M., Quesnel, Y., Rochette, P., Demory, F., Fozing, E. M., Njanko, T., Hippolyte, J. C.,
799 and Affaton, P., 2013, Rock magnetic investigation of possible sources of the Bangui magnetic
800 anomaly: Physics of the Earth and Planetary Interiors, v. 224, p. 11-20.
801 [142] Launay, N., Quesnel, Y., Rochette, P., and Demory, F., 2018, Iron Formations as the Source of the
802 West African Magnetic Crustal Anomaly: Frontiers in Earth Science, v. 6, p. 32.
803 [143] McEnroe, S. A., Robinson, P., Church, N., and Purucker, M., 2018, Magnetism at Depth: A View
804 from an Ancient Continental Subduction and Collision Zone: Geochemistry, Geophysics,
805 Geosystems, v. 19, no. 4, p. 1123-1147.
806 [144] Olsen, N., Ravat, D., Finlay, C. C., and Kother, L. K., 2017, LCS-1: a high-resolution global model
807 of the lithospheric magnetic field derived from CHAMP and Swarm satellite observations:
808 Geophysical Journal International, v. 211, no. 3, p. 1461-1477.
809 [145] Launay, N., Rochette, P., Quesnel, Y., Demory, F., Bezaeva, N. S., and Lattard, D., 2017,
810 Thermoremanence acquisition and demagnetization for titanomagnetite under lithospheric pressures:
811 Geophysical Research Letters, v. 44, no. 10, p. 4839-4845.145
812 [146] Jackson, M., Moskowitz, B., Rosenbaum, J., and Kissel, C., 1998, Field-dependence of AC
813 susceptibility in titanomagnetites: Earth and Planetary Science Letters, v. 157, no. 3, p. 129-139.
814 [147] Dunlop, D. J., and Özdemir, Ö., 1997, Rock magnetism: fundamentals and frontiers, Cambridge,
815 Cambridge University Press, Cambridge Studies in Magnetism, 573 p.

816 [148] Hunt, C. P., Moskowitz, B. M., and Banerjee, S. K., 1995, Magnetic properties of rocks and
817 minerals, in Union, A. G., ed., Rock physics and phase relations: a handbook of physical constants,
818 A.G.U. Reference Shelf 3, p. 189-204.
819 [149] Özdemir, Ö., and Dunlop, D. J., 2014, Hysteresis and coercivity of hematite: Journal of
820 Geophysical Research: Solid Earth, v. 119, no. 4, p. 2582-2594.
821 [150] Martín-Hernández, F., and García-Hernández, M. M., 2010, Magnetic properties and anisotropy
822 constant of goethite single crystals at saturating high fields: Geophysical Journal International, v. 181,
823 no. 2, p. 756-761.
824

Acknowledgements:

This work was supported by the National Science Foundation (grants EAR-0521558 and EAR-1345105 to ECF, EAR-1246921 to DR), National Aeronautics and Space Administration (grants NNX16AN51G and 80NSSC19K0014 to DR) and internal funding from the University of Münster. We acknowledge the editorial assistance of Associate Editors Matthew Gleeson and Laura Zinke, and four anonymous reviewers who greatly contributed to clarify this manuscript.

Contributions:

All authors contributed equally to drafting the figures, table and text.

Online linking:

References:

Figure captions

Figure 1. Earth's lithospheric magnetic field variations. Total intensity magnetic anomaly field model (the part of the field originating from lithospheric magnetic sources) from CHAMP and Swarm magnetic field satellites[144]. Magnetic anomalies have a complex but systematic relationship with the magnetization of their sources depending on the geomagnetic core field intensity and latitude. (See Note 1) Arrows with labels "forearc anomaly" point to subduction zones where expected zones of magnetic slabs, serpentinized mantle wedges, and deep-seated magnetizations of island arcs are found. Arrows with labels "no forearc anomaly" demarcate examples of subduction zones where combination of factors related to slabs (steepness, high plate motion and hence temperatures at depth) result in little magnetic anomaly. Kursk, Bangui, and West Africa are a few of the continental cold cratonic regions of strongest magnetization where some of the magnetization may reside in the mantle. The square in the east-central ancient cold cratonic region of Canada where the base of magnetization was determined at approximately 80 km depth in the uppermost mantle from the North American aeromagnetic database. Yilgarn and Gawler cratons in Australia are some of the other key cratonic regions where magnetization is detected in the mantle. Depending on the magnetic latitude and the intensity of the core magnetic field, anomalies have systematic relationships with respect to magnetic sources. Near both magnetic poles, where the Earth's core magnetic field is near-vertical (roughly >± 70°), magnetic "highs" (reds and whites in Figure 1) result from magnetizations aligned in the direction of the field. If the bulk of the rock's present magnetization were formed during a reversed magnetic epoch, magnetic "lows" form at high latitudes (blues and blacks in Figure 1). Near magnetic equator magnetic "lows" occur over regions of high magnetizations (*e.g.,* Bangui anomaly in Figure 1). The magnetic equator is at approximately 10°N geographic latitude from Africa to Asia and gradually dips to 15°S at the western margin of South America. Because the intensity of the core generated magnetic field is roughly half of that at the pole, the same amount of induced

magnetization in a rock results roughly half the amplitude of magnetic anomalies at the magnetic equator than at both north and source magnetic poles. This is one of the causes of smaller anomaly amplitudes in South America and central to northern Africa. Given this relationship one can understand the exceptional strength of Bangui magnetic anomaly in central Africa and some of the anomaly features in the West African craton.

Fig. 2. Magnetic records from mantle xenoliths. Natural remanent magnetization (NRM) vs. total low-field magnetic susceptibility, *i.e.,* Koenigsberger diagram, for mantle xenoliths showing predicted contributions of the upper mantle to magnetic anomalies[19, 61-62 and unpublished data]. Q_n indicates the Koenigsberger ratio.

Fig. 3. Stability and magnetic properties of the Fe_3O_4 system at upper mantle pressure-temperature conditions. (a) Hematite (α-Fe_2O_3) sample in the diamond anvil cell for the study of magnetic properties by synchrotron Mössbauer spectroscopy at room temperature (bottom) and high temperature (top) upon laser heating. (b) Representative Mössbauer spectra of antiferromagnetic (bottom) and paramagnetic (top) hematite at upper mantle conditions. Solid lines show the theoretical fits, the percentage bars indicate the relative absorptions. (c) Magnetic boundaries in the Fe_3O_4 system. The breakdown of Fe_3O_4 into (α-Fe_2O_3 (hematite) and Fe_4O_5 is shown by the black line[81]. Brown and green lines indicate the Curie temperature of Fe_3O_4[72], and Néel and Morin transition temperatures of α-Fe_2O_3[23]. The Néel temperature of Fe_4O_5 is too low for this phase to play a role in mantle magnetism and it is not reported for the sake of clarity (see discussion in the text). Blue, light red, and red curves depict, respectively, the pressure-temperature profiles for cold (*e.g.*, Solomon), hot (*e.g.*, North Lesser Antilles), and very hot (*e.g.*, South Chile) subducting slabs[23]. Dashed lines are linear extrapolations of the experimental data. Abbreviations: FM, ferromagnetic; PM, paramagnetic; AFM, antiferromagnetic; cAFM, antiferromagnetic with spin canting.

889

890 **Figure 4. Depth to base of magnetization analysis of magnetic data.** (a) Simulation of a 40 km thick
891 magnetic crust with the magnetic field's fractal parameter, $\alpha = 2$ on a plot of amplitude spectrum of
892 the data (wavelength vs amplitude). Solid lines depict simulated spectral curves successively de-
893 fractalized (see the text) with a range of fractal parameters and dashed lines depict corresponding
894 model curves. The colored solid (orange) and dashed (blue) lines are the best-fitting simulated and
895 modeled spectral curves and the model curves in gray do not fit adequately their respective de-
896 fractalized spectra. (b) Root Mean Square (RMS) misfit between simulated and modeled spectral
897 curves vs fractal parameter of the magnetic field. The best-fitting curves are usually near the minima
898 (the RMS misfit is computed from a larger range of wavelengths than shown in these enlarged
899 diagrams of the spectral peak region – the fit near the peak is one of the key criteria). The black curve
900 (the model simulation) shows that the RMS misfit is minimum near $\alpha = 2.1$ and it leads to a derived
901 depth to the base of magnetization of 41 km (which is within 1 km of its true value). (c) The base of
902 magnetization (78 ± 4 km) from the aeromagnetic data in the Archean eastern Superior Craton in
903 Canada (see Figure 1 for location) using the visual best-fitting curves. The best-fit spectral curves are
904 obtained for $\alpha \sim 1.8$-1.9 which are also close to the minimum on the red misfit curve for this region in
905 part (b). The curves below the orange curves are over-corrected from the point of view of fractal
906 corrections (one characteristic of identifying this is that they lead to the depth to the top of the layer in
907 the air).

908

909 **Fig. 5. The magnetic mantle.** Schematic cross-section showing magnetic sources in the upper mantle in
910 different tectonic settings associated with low geotherm regions. Note that the oceanic crust is
911 generally ≤6 km thick.

Alt-S%
This parameter quantifies the degree of sulfide alteration in percent and is the total Fe-hydroxide area divided by the total sulfide area (including Fe-hydroxide) obtained by point counting[71]. This parameter is also a proxy for mantle rock alteration, which is used in petromagnetic studies to determine if the NRM of a mantle xenolith has been chemically modified.

Blocking temperature
At low temperatures, the thermal energy becomes smaller and the magnetic moments become blocked. This temperature is the blocking temperature.

Bouguer gravity anomaly
The gravity field variation obtained from gravity observations in order to remove the effect of topographic and bathymetric variations, which involve some of the largest density contrasts in the crust and upper mantle and thus reflect the effect of topography/bathymetry. The correction allows one to assess subsurface geologic mass variations and isostatic compensation of topographic masses.

Canted antiferromagnetism
A type of magnetic ordering characterized by a non-zero magnetic moment in antiferromagnetic materials. The magnetic moment is caused by spins being tilted by a small angle about their axis ("canted") rather than being exactly co-parallel. In hematite, this effect occurs above the Morin-transition temperature.

Cratonic (non-cratonic) setting
Cratonic setting refers to a geologically stable large region in continental areas that were consolidated by plate tectonic processes. Conversely, non-cratonic settings are areas that are marginal to cratonic areas or that may have been tectonically active in relatively recent times.

Curie (Neél) temperature, T_c (T_N)
Temperatures above which ferrimagnetic (for T_N, ferromagnetic/antiferromagnetic) coupling causing spontaneous magnetization is randomized and destroyed, resulting in the material becoming paramagnetic.

Curie depth
The Curie depth is the depth below the Earth's surface where ferrimagnetic/ferromagnetic minerals in rocks abruptly lose their spontaneous magnetization as a result of exceeding their Curie temperature. This depth is typically inferred from spectral analysis of near surface magnetic data and in ideal circumstances from inversion of aeromagnetic/satellite data.

De-fractaled amplitude spectra
Amplitude spectrum of magnetic anomalies where the power-law dependence is removed[102, 107]

De-fractaling
Removal of power-law (or fractal) characteristics from observed spectra having power-law characteristics.

Ferromagnetism

Alt-S%
This parameter quantifies the degree of sulfide alteration in percent and is the total Fe-hydroxide area divided by the total sulfide area (including Fe-hydroxide) obtained by point counting[71]. This parameter is also a proxy for mantle rock alteration, which is used in petromagnetic studies to determine if the NRM of a mantle xenolith has been chemically modified.

Blocking temperature
At low temperatures, the thermal energy becomes smaller and the magnetic moments become blocked. This temperature is the blocking temperature.

Bouguer gravity anomaly
The gravity field variation obtained from gravity observations in order to remove the effect of topographic and bathymetric variations, which involve some of the largest density contrasts in the crust and upper mantle and thus reflect the effect of topography/bathymetry. The correction allows one to assess subsurface geologic mass variations and isostatic compensation of topographic masses.

Canted antiferromagnetism
A type of magnetic ordering characterized by a non-zero magnetic moment in antiferromagnetic materials. The magnetic moment is caused by spins being tilted by a small angle about their axis ("canted") rather than being exactly co-parallel. In hematite, this effect occurs above the Morin-transition temperature.

Cratonic (non-cratonic) setting
Cratonic setting refers to a geologically stable large region in continental areas that were consolidated by plate tectonic processes. Conversely, non-cratonic settings are areas that are marginal to cratonic areas or that may have been tectonically active in relatively recent times.

Curie (Neél) temperature, T_c (T_N)
Temperatures above which ferrimagnetic (for T_N, ferromagnetic/antiferromagnetic) coupling causing spontaneous magnetization is randomized and destroyed, resulting in the material becoming paramagnetic.

Curie depth
The Curie depth is the depth below the Earth's surface where ferrimagnetic/ferromagnetic minerals in rocks abruptly lose their spontaneous magnetization as a result of exceeding their Curie temperature. This depth is typically inferred from spectral analysis of near surface magnetic data and in ideal circumstances from inversion of aeromagnetic/satellite data.

De-fractaled amplitude spectra
Amplitude spectrum of magnetic anomalies where the power-law dependence is removed[102, 107]

De-fractaling
Removal of power-law (or fractal) characteristics from observed spectra having power-law characteristics.

Ferromagnetism

Magnetic state of matter when magnetic moments are aligned by magnetic exchange forces. Ferromagnetism is a larger class of magnetic materials with involve different sub-classes called ferrimagnetism, ferromagnetism, antiferromagnetism, canted antiferromagnetism, etc. Within a crystallographic structure, ferromagnetism orders magnetic moments either parallel, antiparallel, or imperfectly antiparallel with respect to each other in the lattice.

Fourier amplitude spectrum
Amplitude of each wavelength of a spatial or time variation arranged according to their wavelength where the wavelengths and amplitudes are obtained through Fourier analysis. It can be represented also by the inverse of the wavelength (called wavenumber or frequency). It reflects the contribution of each wavenumber to the signal and can be one- or multi-dimensional analysis.

Fractal magnetization
Fractal relationship of the magnetization distribution.

Fractal parameter
The exponent associated with the power law that governs the spatial characteristics of magnetization or magnetic anomaly in the context of this review.

Loss on ignition (LOI)
High-temperature (~1,000ºC) heating experiment in inert atmosphere or vacuum designed to quantify the percentage of volatile elements in a rock.

Low-field magnetic susceptibility (K_{lf})
Slope of the magnetization vs applied field curve in magnetic hysteresis when the applied field is sufficiently low to allow reversible magnetization.

Magnetic coercivity (H_c)
In a magnetic hysteresis loop or in-field magnetic experiment, the field applied in opposite direction required to cancel the acquired magnetization.

Morin transition
Magnetic phase transition in hematite (Fe_2O_3) at ~260 K (at ambient pressure). Upon transition the antiferromagnetic ordering is reorganized from being aligned parallel to the crystallographic c-axis below the transition temperature to be aligned perpendicular to the c-axis above the transition temperature that gives rise to canted antiferromagnetism.

Multidomain state (MD)
Magnetic state of a ferrimagnetic (*sensu lato*) mineral that contains multiple (more than 3-4) areas (or domains) within, where magnetization can be considered homogeneous.

Natural Remanent Magnetization (NRM)
It is the total permanent magnetization of a natural rock or specimen recorded in the formation and may include multiple magnetizing episodes and types of remanent magnetization.

Paramagnetism

Magnetic state of matter caused by unpaired electrons in unfilled orbitals of atoms or ions where free magnetic moments do not have magnetic exchange and therefore only align with a magnetic field is applied. In the absence of an external field, magnetic moments are randomly oriented.

Saturation remanent magnetization (M_{rs})
Maximum remanent magnetization reached in an increasingly high applied field experiment. In a hysteresis loop, it coincides with the magnetization when the cycle crosses the field equal to the zero value.

Serpentinization
Geochemical reaction of peridotite with aqueous fluids to form serpentine. This is the most common type of alteration for Earth's mantle materials.

Solid-solution
In this context, considering one mineral phase the solvent and one cation type the solute, the latter is embedded in the solvent lattice such that a continuous range of compositions between end-member compositions can result.

Thermoremanent Magnetization (TRM)
Permanent or remanent magnetization acquired by a ferromagnetic mineral (*sensu lato*) when cooled through its blocking temperature in the presence of a DC magnetic field, most commonly the Earth's Magnetic Field.

Verwey transition
Magnetic phase transition shown by magnetite (Fe_3O_4) at T_v~120K (at ambient pressure). Upon heating, magnetite gradually transforms from a crystallographic monoclinic into an inverse spinel structure.

Xenolith
A foreign rock surrounded by a larger volume of rock. Here, mantle xenolith are deep-seated fragments of the mantle that ascend to the surface while being passively transported by a basaltic or kimberlitic magma.

Magnetic state of matter when magnetic moments are aligned by magnetic exchange forces. Ferromagnetism is a larger class of magnetic materials with involve different sub-classes called ferrimagnetism, ferromagnetism, antiferromagnetism, canted antiferromagnetism, etc. Within a crystallographic structure, ferromagnetism orders magnetic moments either parallel, antiparallel, or imperfectly antiparallel with respect to each other in the lattice.

Fourier amplitude spectrum
Amplitude of each wavelength of a spatial or time variation arranged according to their wavelength where the wavelengths and amplitudes are obtained through Fourier analysis. It can be represented also by the inverse of the wavelength (called wavenumber or frequency). It reflects the contribution of each wavenumber to the signal and can be one- or multi-dimensional analysis.

Fractal magnetization
Fractal relationship of the magnetization distribution.

Fractal parameter
The exponent associated with the power law that governs the spatial characteristics of magnetization or magnetic anomaly in the context of this review.

Loss on ignition (LOI)
High-temperature (~1,000ºC) heating experiment in inert atmosphere or vacuum designed to quantify the percentage of volatile elements in a rock.

Low-field magnetic susceptibility (K_{lf})
Slope of the magnetization vs applied field curve in magnetic hysteresis when the applied field is sufficiently low to allow reversible magnetization.

Magnetic coercivity (H_c)
In a magnetic hysteresis loop or in-field magnetic experiment, the field applied in opposite direction required to cancel the acquired magnetization.

Morin transition
Magnetic phase transition in hematite (Fe_2O_3) at ~260 K (at ambient pressure). Upon transition the antiferromagnetic ordering is reorganized from being aligned parallel to the crystallographic c-axis below the transition temperature to be aligned perpendicular to the c-axis above the transition temperature that gives rise to canted antiferromagnetism.

Multidomain state (MD)
Magnetic state of a ferrimagnetic (*sensu lato*) mineral that contains multiple (more than 3-4) areas (or domains) within, where magnetization can be considered homogeneous.

Natural Remanent Magnetization (NRM)
It is the total permanent magnetization of a natural rock or specimen recorded in the formation and may include multiple magnetizing episodes and types of remanent magnetization.

Paramagnetism

Magnetic state of matter caused by unpaired electrons in unfilled orbitals of atoms or ions where free magnetic moments do not have magnetic exchange and therefore only align with a magnetic field is applied. In the absence of an external field, magnetic moments are randomly oriented.

Saturation remanent magnetization (M_{rs})
Maximum remanent magnetization reached in an increasingly high applied field experiment. In a hysteresis loop, it coincides with the magnetization when the cycle crosses the field equal to the zero value.

Serpentinization
Geochemical reaction of peridotite with aqueous fluids to form serpentine. This is the most common type of alteration for Earth's mantle materials.

Solid-solution
In this context, considering one mineral phase the solvent and one cation type the solute, the latter is embedded in the solvent lattice such that a continuous range of compositions between end-member compositions can result.

Thermoremanent Magnetization (TRM)
Permanent or remanent magnetization acquired by a ferromagnetic mineral (*sensu lato*) when cooled through its blocking temperature in the presence of a DC magnetic field, most commonly the Earth's Magnetic Field.

Verwey transition
Magnetic phase transition shown by magnetite (Fe_3O_4) at T_v~120K (at ambient pressure). Upon heating, magnetite gradually transforms from a crystallographic monoclinic into an inverse spinel structure.

Xenolith
A foreign rock surrounded by a larger volume of rock. Here, mantle xenolith are deep-seated fragments of the mantle that ascend to the surface while being passively transported by a basaltic or kimberlitic magma.

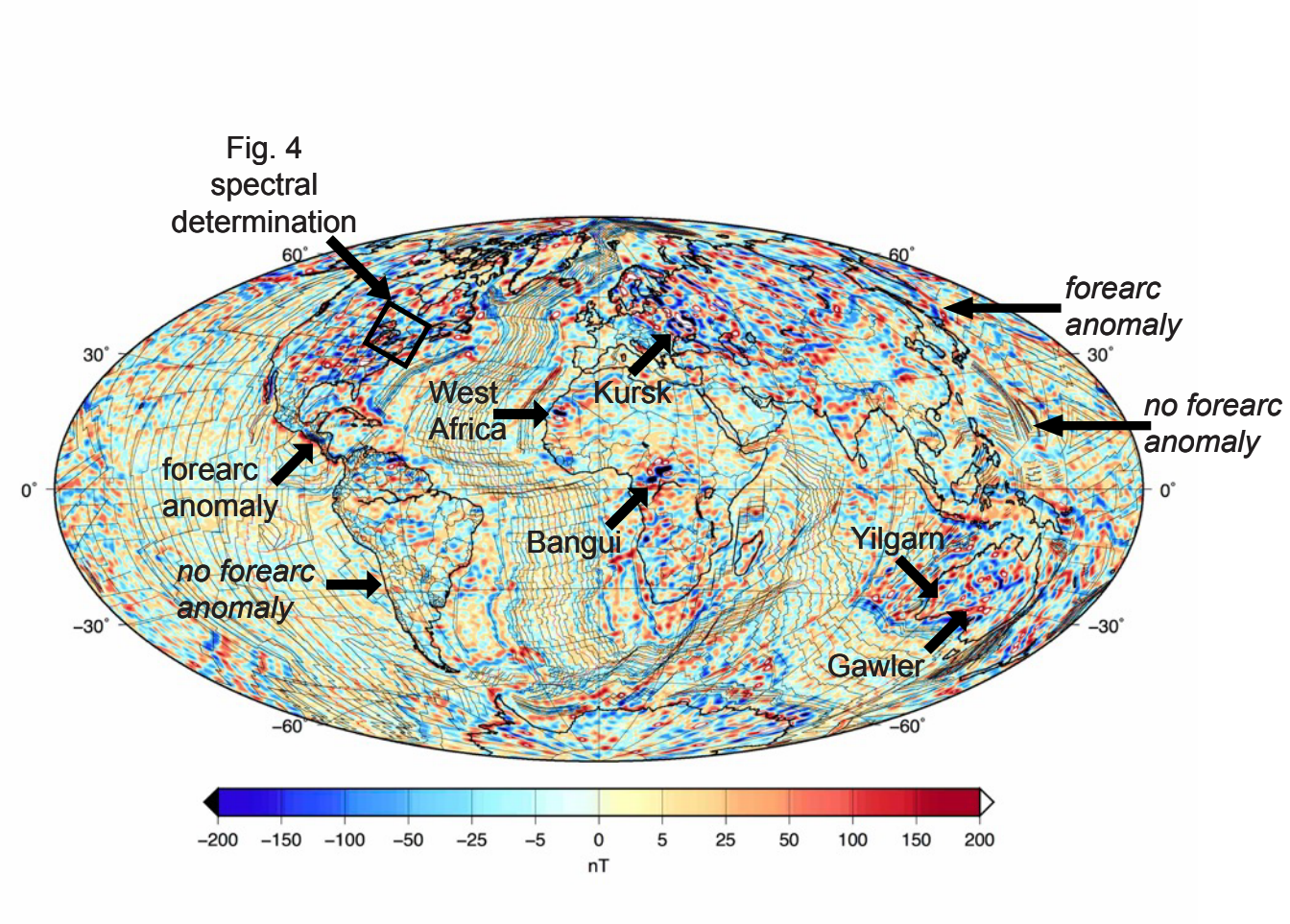
Fig. 4
spectral
determination
60°
30°
0°
−30°
−60°
West
Africa
Kursk
forearc
anomaly
no forearc
anomaly
forearc
anomaly
no forearc
anomaly
Bangui
Yilgarn
Gawler
−200
−150
−100
−50
−25
−5
0
5
25
50
100
150
200
nT

Figure 1

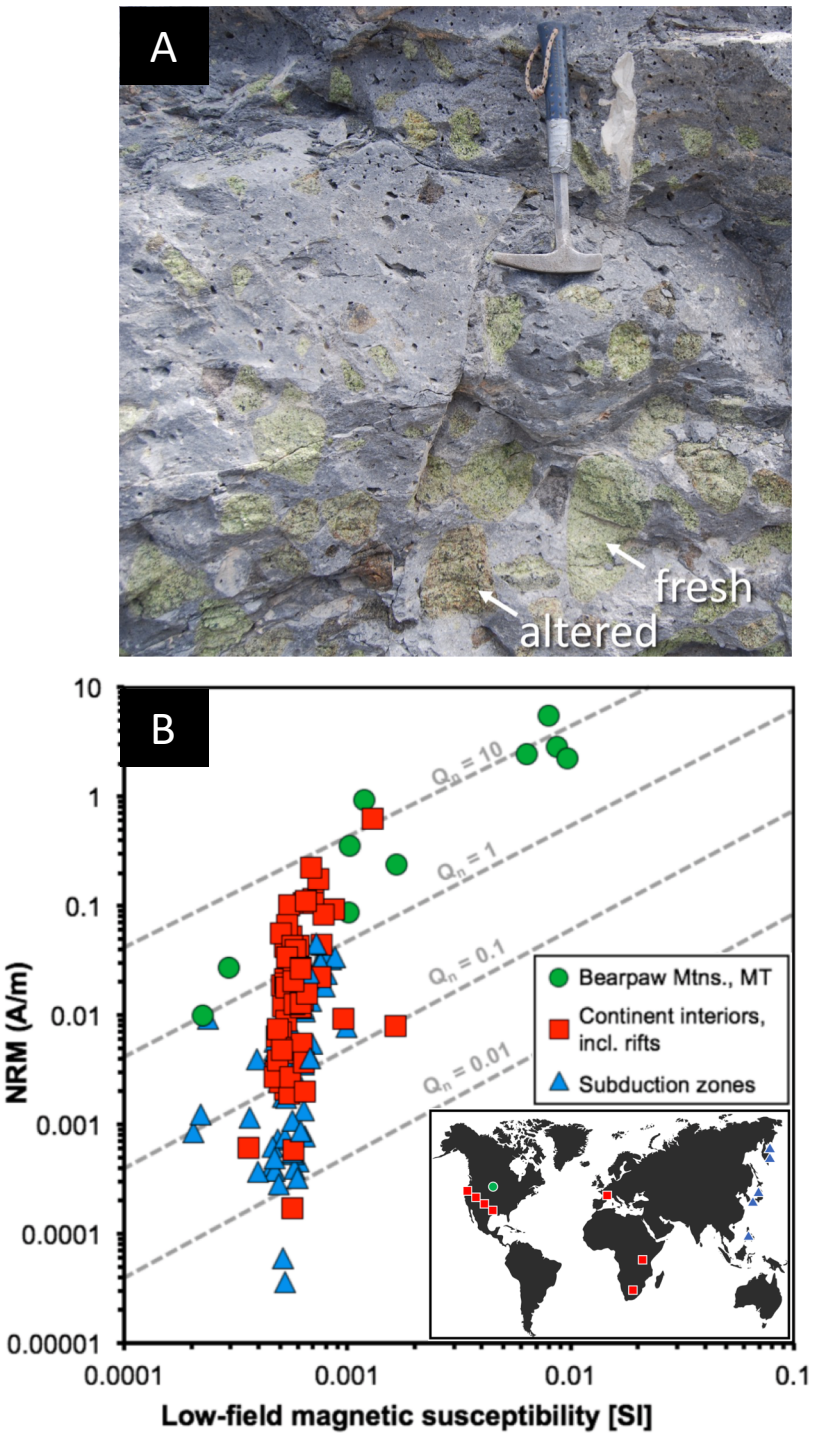
A
fresh
altered
B
10
1
0.1
0.01
0.001
0.0001
0.00001
NRM (A/m)
0.0001
0.001
0.01
0.1
Low-field magnetic susceptibility [SI]
Q_n = 10
Q_n = 1
Q_n = 0.1
Q_n = 0.01
Bearpaw Mtns., MT
Continent interiors, incl. rifts
Subduction zones

Fig. 2.

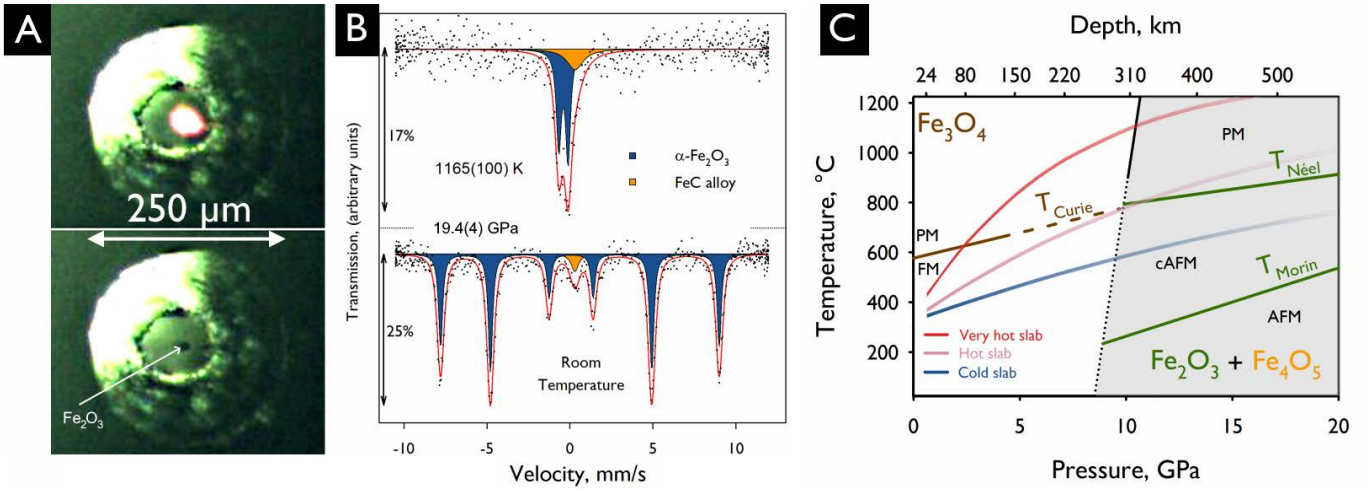
A
250 μm
Fe_2O_3
B
17%
1165(100) K
α-Fe_2O_3
FeC alloy
19.4(4) GPa
25%
Room
Temperature
Transmission, (arbitrary units)
-10
-5
0
5
10
Velocity, mm/s
C
Depth, km
24
80
150
220
310
400
500
1200
1000
800
600
400
200
Temperature, °C
Fe_3O_4
PM
$T_{Néel}$
T_{Curie}
PM
FM
cAFM
T_{Morin}
AFM
Very hot slab
Hot slab
Cold slab
Fe_2O_3 + Fe_4O_5
0
5
10
15
20
Pressure, GPa

Figure 3

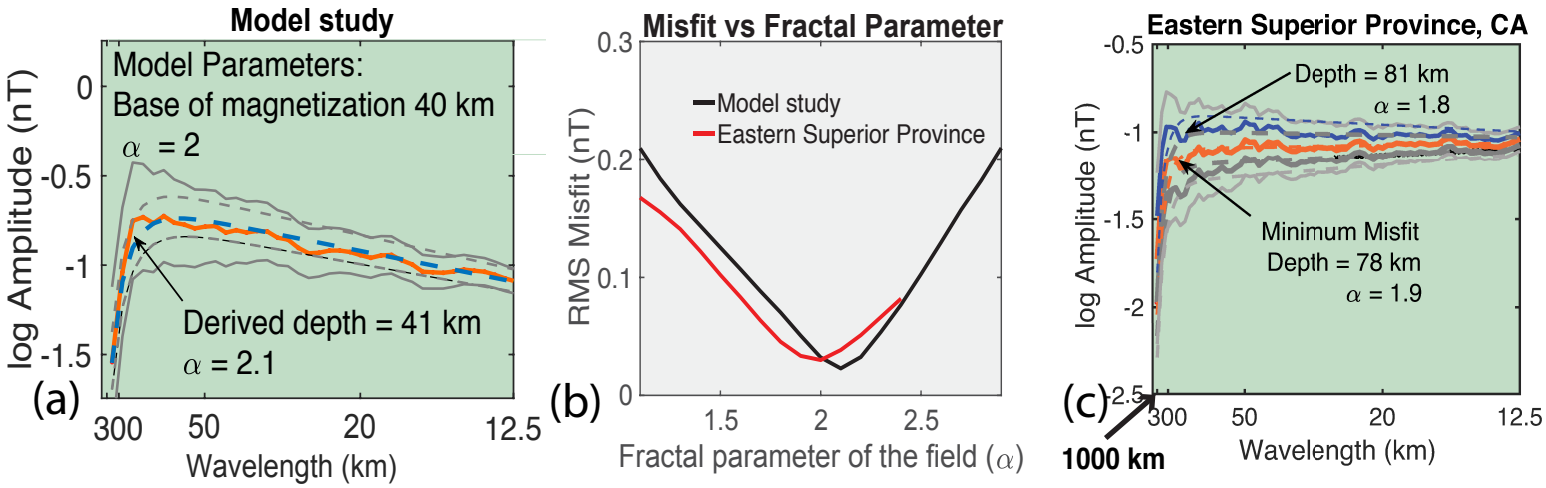
Model study
Model Parameters:
Base of magnetization 40 km
α = 2
Derived depth = 41 km
α = 2.1
log Amplitude (nT)
Wavelength (km)
(a)
Misfit vs Fractal Parameter
Model study
Eastern Superior Province
RMS Misfit (nT)
Fractal parameter of the field (α)
(b)
Eastern Superior Province, CA
Depth = 81 km
α = 1.8
Minimum Misfit
Depth = 78 km
α = 1.9
1000 km
(c)

Figure 4

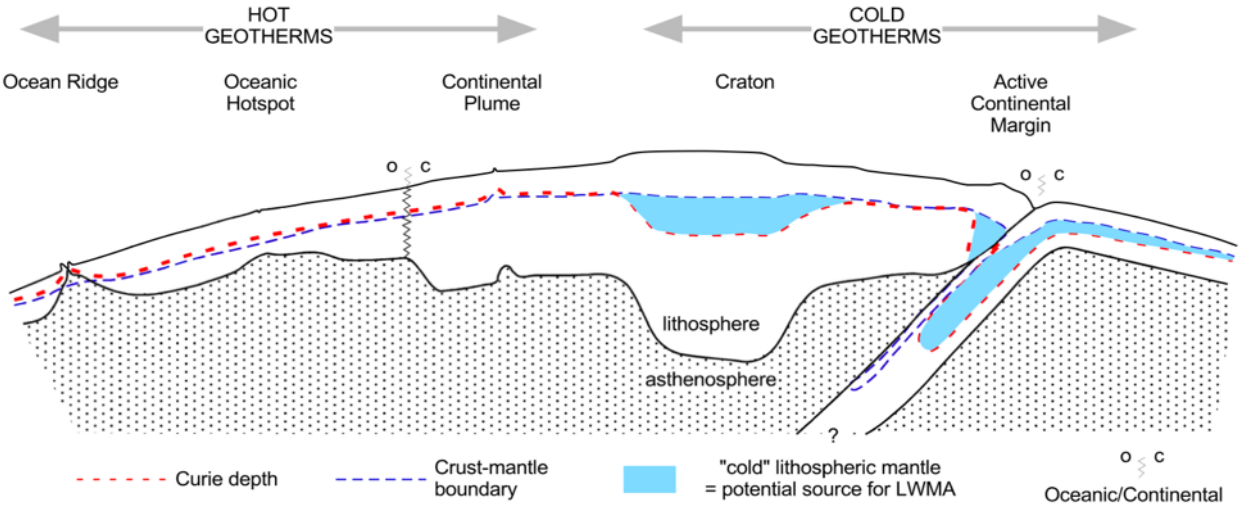
HOT
GEOTHERMS
COLD
GEOTHERMS
Ocean Ridge
Oceanic
Hotspot
Continental
Plume
Craton
Active
Continental
Margin
o c
o c
lithosphere
asthenosphere
?
Curie depth
Crust-mantle
boundary
"cold" lithospheric mantle
= potential source for LWMA
o c
Oceanic/Continental

Figure 5